

University of Vermont

UVM ScholarWorks

Graduate College Dissertations and Theses

Dissertations and Theses

2023

A Duration-Over-Threshold Model For Flood Frequency And Flow Regime Characterization

Kenneth Scott Feasley Lawson
University of Vermont

Follow this and additional works at: <https://scholarworks.uvm.edu/graddis>



Part of the [Civil Engineering Commons](#), [Hydrology Commons](#), and the [Statistics and Probability Commons](#)

Recommended Citation

Lawson, Kenneth Scott Feasley, "A Duration-Over-Threshold Model For Flood Frequency And Flow Regime Characterization" (2023). *Graduate College Dissertations and Theses*. 1779.
<https://scholarworks.uvm.edu/graddis/1779>

This Thesis is brought to you for free and open access by the Dissertations and Theses at UVM ScholarWorks. It has been accepted for inclusion in Graduate College Dissertations and Theses by an authorized administrator of UVM ScholarWorks. For more information, please contact schwrrks@uvm.edu.

A DURATION-OVER-THRESHOLD MODEL FOR FLOOD FREQUENCY
AND FLOW REGIME CHARACTERIZATION

A Thesis Presented

by

Kenneth Scott Feasley Lawson

to

The Faculty of the Graduate College

of

The University of Vermont

In Partial Fulfillment of the Requirements
for the Degree of Master of Science
Specializing in Civil and Environmental Engineering

October, 2023

Defense Date: September 1, 2023
Thesis Examination Committee:

Kristen L. Underwood, Ph.D., Advisor
Rebecca M. Diehl, Ph.D., Chairperson
Donna M. Rizzo, Ph.D.
Holger Hoock, DPhil, Dean of the Graduate College

Abstract

Proper characterization of river flow is essential for the development of structural and non-structural measures to reduce flood damages, restore ecosystem functions, and manage environmental contaminants in riparian zones. In particular, the duration of flood events is an important feature of floods that drives riverine processes such as erosion, geomorphic adjustment, habitat suitability, nutrient and water quality dynamics, and structural damage. Despite this, most flood characterization methods focus solely on relating the magnitude of annual-maximum discharges to frequency, without addressing the duration of flood events. We investigated event-specific discharge-duration dynamics at 33 USGS stream gages within the US state of Vermont. Building on the method of Feng et al. 2017, flood events from 15-minute discharge timeseries were extracted using an automated threshold method, and a statistical model was fit at each gage for both frequency of discharge exceedance and conditional duration of discharge exceedance. This Duration-Over-Threshold model can estimate the arrival rate of a flowrate threshold, q , being exceeded for a given duration, d . Fitted model parameters were compared to basin and channel physiographical characteristics to develop regional regression equations and examine potential watershed processes underlying the duration dynamics. Flood duration and hydrograph rate of recession were found to be best predicted by drainage area, mainstem slope, and soil depth/type. The regional regression equations enable design event estimation in ungauged catchments of the study region, which may be used to improve the predictive capacity of hydraulic and ecosystem models, outline a range of potential geomorphic trajectories, or inform emergency management plans and flood damage rating curves.

Acknowledgements

My arrival at this point has not been a story of rugged individualism. Rather, this current summit reflects a culmination of support, encouragement, and inspiration that many groups and individuals have given me throughout my life. I am grateful to all these people, and I would like to name a few now. Let me begin with my parents and sister. They showed me the joys of learning and provided me with an education to problem-solve, examine the world, and discuss it with others. Of that education, I owe it to my undergraduate professors Steven Loheide and David Bohnhoff for providing me with very enjoyable experiences in research. Without these two, I never would have considered returning to graduate school.

Thank you to Scott Hamshaw for the serendipitous email-forward that led me to coming to the University of Vermont (UVM). I am grateful to the entire Civil and Environmental Engineering department here for the community and thought-provoking discussion they have given me for the past two years. Specifically, I should thank Ali Dadkhah, Shaurya Swami, and Mitch Joseph for weekly coffee and nerd-out sessions; Dustin Kincaid for helping make Burlington my new home and guiding me through my first years in academia; Ryan Van Der Heijden, Bijay KC, Bobby Worley, Lindsay Worley, and Jeremy Matt for being excellent officemates and collaborators; and Evan Fitzgerald, Roy Schiff, Mike Kline, and Evelyn Boardman for guiding and assisting me on a project I will be proud of for years to come.

I'm thankful for the many friends both near and far, whose adventures, phone calls, and quality time have kept me smiling. Thank you as well to the land in Vermont for

providing me complexity to study, mountains and water for hiking and swimming, and many paths to become lost in thought on.

Finally, and most importantly, I am forever indebted to my advisors (both official and unofficial). Kristen Underwood has given me new vocabulary and lenses with which to view rivers and has provided consistent encouragement, feedback, and insight. Rebecca Diehl has pushed me to think deeper on so many topics, is one of my favorite people to workshop ideas and collaborate with, and has provided invaluable feedback throughout this project and others. Beverley Wemple has given me support and mentorship from my very first interview through starting a new job at UVM. Finally, Donna Rizzo has given me tools and a worldview to last a lifetime. Gaining an ability to visualize and think about multidimensional data has truthfully been one of the great joys of my time in graduate school. I thank her for the education and constant support and encouragement for the past two years.

Table of Contents

Abstract.....	i
Acknowledgements.....	ii
Chapter 1 Comprehensive Literature Review.....	1
Chapter 2 The Duration-Over-Threshold Model.....	12
2.1 Introduction.....	12
2.2 Methods.....	17
2.2.1 Model Formulation.....	17
2.2.2 Streamflow Records and Data Processing.....	22
2.2.3 Model Regionalization.....	25
2.4 Results & discussion.....	27
2.4.1 Model Performance.....	27
2.4.6 Model Regionalization.....	34
2.5 Conclusions.....	41
2.6 Supplementary Information.....	43
2.6.1 Missing Data Handling.....	46
2.6.2 Model Derivation.....	43
2.6.3 Catchment and Reach Physiographic characteristics.....	49
2.6.4 Skew Isoline Map.....	57
Chapter 3 Concluding Remarks.....	59
Comprehensive Bibliography.....	62

List of Figures

Figure 1-1 Reproduction of schematic from Gaál et al. (2012).....	3
Figure 1-2 Text from Fuller (1914).....	5
Figure 1-3 Flow-duration curve	6
Figure 1-4 Summary of N-day flood	7
Figure 1-5 Joint distribution.....	8
Figure 2-1. Graphical workflow.....	17
Figure 2-2 Fitted model.	21
Figure 2-3 Study area.....	23
Figure 2-4 Marginal distribution.....	27
Figure 2-5 QQ plots of event duration.....	29
Figure 2-6 Comparison of Power Law exponential decay.....	31
Figure 2-7 Power law regression	32
Figure 2-8 Duration of the 10-year exceedance of bankfull depth.	33
Figure 2-9 Imputation summary.....	48
Figure 2-10 Regional skew map.	57

Chapter 1 | Comprehensive Literature Review

Flood duration drives the outcomes of numerous river processes, but methods to characterize this component of river flow regime are underdeveloped. Geomorphic effectiveness studies have shown that duration above a flowrate threshold is more important than peak discharge in determining the type and amount of erosion during flood events (Costa & O'Connor, 1995; Gervasi et al., 2021; Lekach & Enzel, 2021; Magilligan et al., 2015; Wolman & Miller, 1960). Flood damages to property are sensitive to flood duration (FEMA, 2006; Merz et al., 2013; Soetanto & Proverbs, 2004; Thielen et al., 2005), and duration is an important consideration for emergency response plans (Pfurtscheller & Schwarze, 2008). Ecologists have long noted that the amount of time a fluvial landform is inundated is a vital component of ecological gradient and determines plant distributions (Acosta & Perry, 2001; Arias et al., 2012; Bedinger, 1979; Ferreira & Stohlgren, 1999; Hupp & Osterkamp, 1985; Junk et al., 1989). Increasing the length of time river waters are in contact with reactive floodplain surfaces can influence water quality and watershed nutrient retention in floodplain reconnection studies (Baustian et al., 2019; Newcomer Johnson et al., 2016). Properly characterizing the duration component of a river's flow regime could therefore significantly improve predictive modeling of these processes.

Beyond advancing our ability to predict river processes, improved characterization of river flow duration holds promise for cutting through the complex behavior of watershed systems. Spatial heterogeneity, process interaction, and nonlinearity make it challenging, if not impossible, for physically based models such as Darcy's law, the Richards equation,

or the Saint-Venant equations to predict the behavior of an entire watershed (Baker & Gollub, 1996; McDonnell et al., 2007; Sivapalan, 2003). The shortcomings of this bottom-up approach have been a stumbling block for the science of watershed hydrology, but progress is not doomed (Sivapalan, 2009; Sivapalan et al., 2003). In the words of science historian James Gleick, “Of all the possible pathways of disorder, nature favors just a few,” and incorporating methods from adjacent sciences such as statistics, complex systems, or ecology – which were developed for discerning pattern from complexity – paves a path for advancing our hydrologic understanding (Hrachowitz et al., 2013; McDonnell et al., 2007; Ottino, 2003).

Borrowing from ecology, the functional trait framework suggests that instead of interrogating large amounts of physical and process heterogeneity, examining their net result (traits) is sufficient (Diehl et al., 2017; Funk et al., 2017; McDonnell et al., 2007). Novel characterizations of river flow regime, such as the “flood timescale” of Gaál et al. (2012), are prime examples of such traits. In their words, this trait “acts like a fingerprint of a catchment because it incorporates many aspects of runoff generation such as soils, geology, slope, and land use, precipitation amount and duration, timing of peak rainfall intensity, and antecedent precipitation.” Once functional traits are defined and measured, they may be linked to both causal processes – such as climate, geomorphology, or dominant flow mechanism – and effective processes – such as ecology, sediment transport, or water chemistry – to reveal reproducible patterns and deepen our system understanding (Gaál et al., 2012; Hrachowitz et al., 2013; McDonnell et al., 2007; Sivapalan, 2003). For example,

Gaál et al. (2012) used a comparative hydrology approach to develop the conceptual model of flood duration causal processes shown in Figure 1-1.

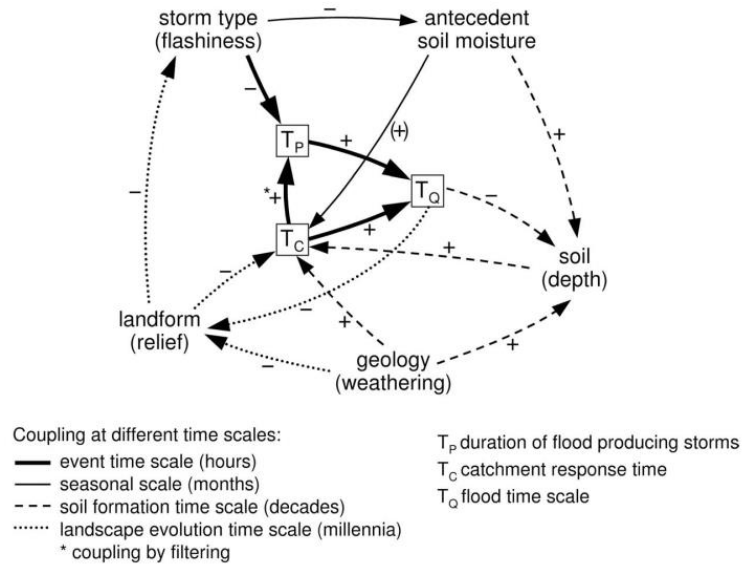


Figure 1-1 Reproduction of schematic from Gaál et al. (2012) showing the coupling of process controls on the flood timescale based on a comparative analysis. Plus and minus signs indicate whether coupling is positive or negative.

Despite the potential benefits of characterizing flood duration, a large portion of hydrologic studies remain focused on a view of flow regime outlined over one hundred years ago – statistical Flood Frequency Analysis (FFA). In December 1914, Weston E. published a paper titled *Flood Flows* that fully embraced the idea that watershed heterogeneity and process complexity were too great to be modeled discretely (Fuller, 1914). Instead, he suggested that the whole problem be handled with statistics (his words replicated in Figure 1-2). This paper along with a 1930 paper from Fuller’s collaborator Allen Hazen kickstarted the science of FFA and outlined most of its paradigms and problems (Hazen, 1930). Most notably, the papers presented the idea of the annual-maximum flood and developed statistical methods to relate flood magnitude to recurrence

interval (although this point was hotly contested by Robert E. Horton, who, in his review of the article, claimed he had been relating discharges to frequency with another engineer since 1896). Between Hazen and Fuller's two papers they discussed ideas ranging from the utility and limitations of gage data in representing future conditions, hydrologic nonstationarity, the physical characteristics driving flood magnitude, the potential benefits of probabilistic rainfall models coupled with physically-based runoff models, floodplain management, engineering economic analysis, and the challenge of using annual-maximum floods in arid regions. While this is not a comprehensive list of the outstanding problems in FFA today, it is near to it.

While FFA has been instrumental in designing infrastructure, managing flood hazards, and supporting scientific inquiry to river functions, its paradigm and challenges are now over 100 years old. FFA methods have evolved with time, but some methods have become so commonplace as to be written into legislation and endorsed at the federal level (Benson, 1968; Dawdy et al., 2012; FEMA, 2019; Kidson & Richards, 2005). Many prominent FFA researchers agree that advances in the statistical methods underlying this science are reaching a point of diminishing returns and that future progress will come from utilizing the functional traits of a rivers flood frequency curve to infer process (Dawdy et al., 2012). We suggest that incorporating elements of flood duration into these traits could be an equally fruitful next step.

The conditions which produce or affect floods may be divided into two classes: First, those which relate to one stream and tend to make all floods on it greater or less than on others; and second, those which are general in their effect, as far as area is concerned, but are variable in time, tending to produce floods of various magnitudes from time to time.

In the first class may be included the following: The prevailing conditions of rainfall; the size, shape, and slope of the catchment area; the character of the soil and vegetation on the catchment area; the physical characteristics of the stream channel; the storage capacity in reservoirs; and many other physical characteristics of the catchment area and the stream itself. Some of these characteristics may be changed in time by the action of the elements or by the works of man; otherwise, their effect on floods may be considered as constant.

In the second class may be included the following: The rate of rainfall; the snow conditions; the temperature conditions; the quantity of water stored in reservoirs, lakes, and ground at the time the flood occurs; the velocity and direction of the storm; the formation of ice dams or other temporary obstructions in the river; and the many other elements which cause one flood to differ from another on the same stream.

No two floods are exactly alike. Two storms of like intensity, velocity, and direction passing over a catchment area may produce different floods. One coming at a time when the water in the ground and in the lakes and reservoirs is low may produce only a moderate flood. A second, coming at a time when the lakes, reservoirs, and ground are filled, may produce a large flood; or, if the second occurs in conjunction with high temperature, when there is a large quantity of snow on the water-shed, a very large flood may occur.

When the great variety of conditions which affect each flood is considered, it will be seen that the number of combinations which may occur is infinite. When many conditions tending to large floods occur coincidentally with great rainfall, extraordinary floods are produced. The chances of such a coincidence may be considered equal for different streams. Clearly, the study of the effect of elements of this class is one in probabilities.

Figure 1-2 Text from Fuller (1914) outlining the justification for treating watersheds as stochastic instead of deterministic systems.

Of the existing duration characterizations, the flow-duration curve (Figure 1-3) is often used. This curve defines the average percent of time within a year that a river flowrate is exceeded (Olson, 2002; USACE, 2022; Ward & Moran, 2016). The curve may be used to estimate sediment yields, model channel-forming processes, or assess components of ecosystem health (Diehl et al., 2020; Ward & Moran, 2016; Wolman & Miller, 1960). The utility of flow-duration curves, however, is limited by their focus on annual cumulative duration instead of event-specific duration. A parcel inundated for 24 days each year would favor different plant species than a parcel inundated for 24 hours every other week (Auble et al., 1994). Furthermore, Magilligan et al. (2015) observed that event-specific duration, not cumulative duration, controlled the character of geomorphic adjustment in Northeastern US catchments (a short-duration high-energy flood leads to avulsion and sedimentological effects instead of erosive, channel-widening effects). Finally, flow-duration curves are less useful for modeling systems such as detention basins or lakes, where quantity of water over periods shorter than a year control system behavior.

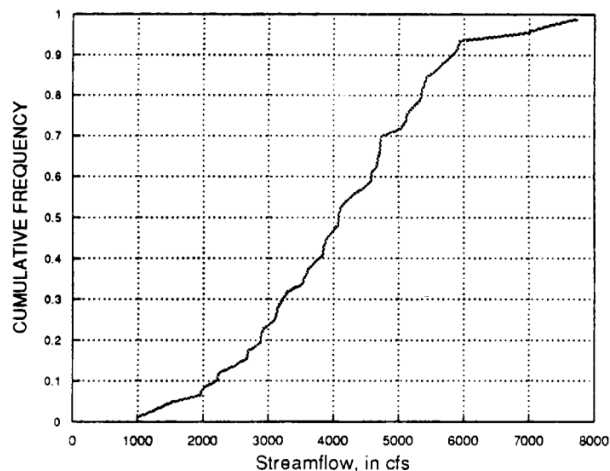


Figure 1-3 Flow-duration curve of Licking River at Catawba, Ky., 1929-1983 reproduced from (Hirsch et al., 1993)

Another conceptualization of flood duration is a moving window used to resample the flowrate timeseries. Various parameters may be tracked in the resampling process and summarized similarly to intensity-duration-frequency (IDF) curves used in rainfall prediction (Figure 1-4) (Frederick et al., 1977; Smith, 1993). Investigations in this vein are commonplace across the scientific literature under various names: flow-duration-frequency, volume-duration-frequency, n-day flood, etc. (Cunderlik & Ouarda, 2006; Devulapalli, 1995; Javelle et al., 2003; Kennedy et al., 2015; Lamontagne et al., 2012; Sherwood, 1994). These analyses are typically used in the design and modeling of storage-based systems such as reservoirs, lakes, and retention basins. Unfortunately, in the process of providing mean discharge over a duration, this model loses information on whether a specific flowrate threshold has been crossed at some point within the window. This limits model utility in some applications. For example, many geomorphic processes have critical flowrate thresholds that may not be accounted for in these kinds of models. Additionally, non-averaged flowrates are necessary to predict the inundation extents that are useful in assessing property damage and floodplain connectivity.

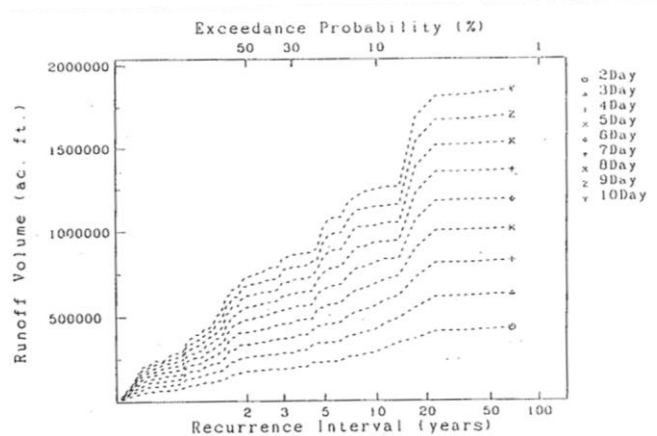


Figure 1-4 Summary of N-day flood characteristics for a watershed in Texas reproduced from Devulapalli (1995)

Copula methods are also used to model the frequency of flood duration, and they have risen in popularity sharply in the last 20 years. Copula methods involve fitting marginal distributions to a set of variables of interest and modeling their dependence structure using one or more copula functions (Genest & Favre, 2007). These models are similar to multivariate distribution models, such as those used by Yue et al. (2001), in that they are joint distributions of any two random variables (Figure 1-5); however, they allow the hydrologic modeler freedom in selecting marginal distribution forms as well as providing several options for modeling the dependence structure of the random variables.

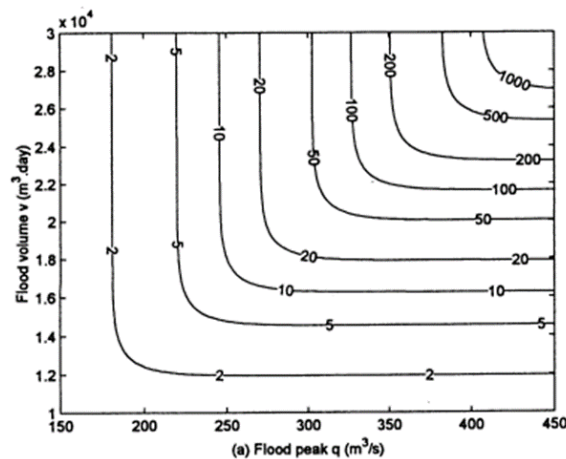


Figure 1-5 An example of the results of a joint distribution analysis reproduced from Yue et al. (2001). Isolines and their labels reflect events with the same return period but different characteristics. This image depicts a multivariate distribution, but copula models would yield similar summary information.

Copulas were first applied in the hydrologic sciences in the mid-2000's by Favre et al. (2004), and the flexible model has been applied in a variety of hydrologic systems since. Bivariate copulas have been used to model pairwise combinations of peak discharge, duration, volume, and time to peak (Bačová Mitková & Halmová, 2014; Razmkhah et al.,

2022; Sraj et al., 2015). Vine copulas have allowed for the modeling of more than two random variables (Amini et al., 2022; Ganguli & Reddy, 2013; Tosunoglu et al., 2020). Copulas have even been used to derive design flood hydrographs (Drobot et al., 2021; Goswami, 2022). When copulas are used to model both discharge and duration, discharge typically reflects the peak discharge of a flood event, and duration typically reflects the time between start and stop of flood quickflow. While these two metrics provide a good estimate of hydrograph shape, the hydrograph ordinates between baseflow and flood peak must be interpolated. A model that specifically characterizes the amount of time spent above intermediate thresholds could yield more accurate information for processes that are dependent on time spent above an intermediate threshold.

Another class of models treats event duration as a conditional probability on flowrate threshold exceedance (Correia, 1987; Feng et al., 2017; USEPA, 2008). By discretizing both flowrate threshold and event-specific duration, these models overcome the shortcomings of the three previous models. Correia (1987) developed a twist on peaks-over-threshold modeling where instead of fitting a distribution to the series of peak flowrates over the truncation threshold, they fit a distribution to the series of truncation threshold exceedance durations. Correia fit this kind of distribution at three truncation thresholds for each of 12 watersheds in Portugal. While this approach allows for estimation of event-specific duration, it is only applicable at those three pre-defined flowrate thresholds. Feng et al. (2017) performed an annual-maxima series (AMS) stage frequency analysis and then parameterized a conditional distribution of exceedance duration for any stage. Their conditional distribution parameterization was comprised of an event mean

duration vs stage relationship and an exponential distribution around each event mean duration. As compared to Correia's three thresholds, Feng's duration-stage relationship enables the modeler to estimate duration at any intermediate stages. Feng's relationship was also developed to work for both riverine gages and gages influence by tidal action. Feng et al. (2017) fit their proposed model at one estuary gage, one tidal gage, and two riverine gages in the Mid-Atlantic region of the United States.

In this thesis, I build upon the strengths of Feng's model but suggest a few refinements for its use in riverine settings. The annual-maxima approach is biased low for frequent events, events that we know drive the bulk of in-channel geomorphic and ecological processes (Karim et al., 2017; Pan et al., 2022). Feng also used a stage timeseries instead of a flowrate timeseries. While a stage-based model will give the best representation of that information for a given gage, discharge is more easily regionalized for inter-basin comparisons and can be predicted given remotely sensed basin characteristics. Lastly, because they only analyzed two riverine sites it is unclear whether the conditional distribution formulation used by Feng can adequately describe flowrate-duration-frequency relationships at riverine sites across a broader region.

This thesis codifies the Duration-Over-Threshold model, a parametric hierarchical statistical model inspired by Feng et al. (2017) that characterizes the return period of a given flowrate threshold being exceeded for a given duration. The objectives of this study are to 1) tailor the model of Feng et al. to frequent events (average recurrence less than 10 years) that we expect drive the bulk of geomorphological and ecohydrological processes (Karim et al., 2017); 2) refine and validate the structure of this model by fitting it at 33

stream gages across the US state of Vermont; 3) relate the model parameters to catchment and reach physiographic characteristics, so that a regional model may be developed for use in ungauged hydrology; 4) provide tractable equations and computer software to enable the use of this model by river practitioners; and 5) present novel functional traits that summarize flood duration dynamics of flow regime in rivers of our Northeast US study area. In this process we hope to answer the following research questions:

- What is the relationship between threshold discharge and duration above that discharge for stream gages in Vermont?
- What is the best statistical distribution to represent flood duration over a threshold?
- What aspects of river flow regime are reflected within the model parameters?
- Which catchment and reach physiographic characteristics best predict model parameters, and can they tell us anything about some physical processes underlying the flow regime?

Chapter 2 | A Duration-Over-Threshold Model for Flood Frequency and Flow Regime Characterization

2.1 Introduction

Flood duration drives the outcomes of numerous river processes, but methods to characterize this component of river flow regime are underdeveloped. Geomorphic effectiveness studies have shown that duration above a flowrate threshold is more important than peak discharge in determining the type and amount of erosion during flood events (Costa & O'Connor, 1995; Gervasi et al., 2021; Leenman et al., 2023; Lekach & Enzel, 2021; Magilligan et al., 2015; Wolman & Miller, 1960). Flood damages to property are sensitive to flood duration (FEMA, 2006; Merz et al., 2013; Soetanto & Proverbs, 2004; Thielen et al., 2005), and duration is an important consideration for emergency response plans (Pfurtscheller & Schwarze, 2008). Ecologists have long noted that the amount of time a fluvial landform is inundated is a vital component of ecological gradient and determines plant distributions (Acosta & Perry, 2001; Arias et al., 2012; Bedinger, 1979; Ferreira & Stohlgren, 1999; Hupp & Osterkamp, 1985; Junk et al., 1989). Increasing the length of time river waters are in contact with reactive floodplain surfaces can influence water quality and watershed nutrient retention in floodplain reconnection studies (Baustian et al., 2019; Newcomer Johnson et al., 2016).

Despite the benefits of comprehensive flow regime characterization, specifically the apparent need to account for flood duration, data are often limited and narrowly focused. Statistical Flood Frequency Analyses (FFA) have historically focused on a single

flood characteristic – peak discharge (Dawdy et al., 2012; England Jr et al., 2019; FEMA, 2019; Fuller, 1914). These types of analysis are widely available on both river and regional levels across the United States. Because the magnitude of discharge describes much of the variability in river processes, and is important for flood inundation extents, flood velocity, and other river dynamics, estimated discharge return periods have been an invaluable tool for hydrologists. The choice of a single characteristic, however, is unnecessarily limiting, and there have been numerous calls to develop novel functional traits of watersheds that represent the culmination of many processes (McDonnell et al., 2007; Sivapalan, 2003). Comparative hydrology approaches may be used to link these functional traits to watershed function (as in the case of Gaál et al. (2012) for duration) and represent a viable path towards advancing our ability to more robustly represent the full flow regime in watershed hydrology studies (Hrachowitz et al., 2013; McDonnell et al., 2007; Sivapalan, 2009; Sivapalan et al., 2003).

Various methods have been presented over the years to quantify different components of flow regime and flood duration. Flow-duration curves define the average percent of time within a year that river flowrate exceeds a threshold discharge (Olson, 2002; USACE, 2022; Ward & Moran, 2016), and they have been used to estimate sediment yields, model channel-forming processes, or assess components of ecosystem health (Diehl et al., 2020; Ward & Moran, 2016; Wolman & Miller, 1960). Moving window analyses are commonplace in the scientific literature under different names (flow-duration-frequency, volume-duration-frequency, n-day flood, etc.) (Cunderlik & Ouarda, 2006; Devulapalli, 1995; Javelle et al., 2003; Kennedy et al., 2015; Lamontagne et al., 2012; Sherwood, 1994;

USEPA, 2008), and this approach is well-suited to the design and modeling of storage-based systems such as reservoirs, lakes, and retention basins. Copulas and other multivariate statistical methods have been used to model river confluence joint flood frequency, design flood hydrographs, and droughts, and they are competent at relating the behavior of multiple random variables such as discharge and duration (Amini et al., 2022; Bačová Mitková & Halmová, 2014; Drobot et al., 2021; Favre et al., 2004; Ganguli & Reddy, 2013; Genest & Favre, 2007; Goswami, 2022; Razmkhah et al., 2022; Sraj et al., 2015; Tosunoglu et al., 2020; Yue et al., 2001). While these methods are incredibly useful for some applications, none sufficiently characterize – on an event basis – a river’s relationship between threshold flowrate and the amount of time spent over that flowrate.

A fourth class of models treats event duration as a conditional probability on flowrate threshold exceedance (Correia, 1987; Feng et al., 2017). Correia (1987) developed an alternative peaks-over-threshold approach where instead of fitting a distribution to the series of peak flowrates over the truncation threshold, they fit a distribution to the series of truncation threshold exceedance durations. Feng et al. (2017) used a similar hierarchical model, but instead of fitting duration distributions at discrete flowrate thresholds, they included a regression that parameterizes the duration distribution as a function of river stage. By discretizing both flowrate threshold and event-specific duration, Feng et al. (2017)’s model is able to estimate the frequency with which a given stage will be exceeded for a certain duration.

Given its many strengths, we adopt this approach and propose several modifications to improve its accuracy and useability in riverine settings. Feng et al. (2017) used daily

mean values to fit their model, but higher-frequency data could yield better flow regime characterization for smaller rivers. While their stage-based model will give the best representation of inundation information for a given river, discharge is more easily regionalized to facilitate cross-basin comparisons and can be predicted given remotely sensed basin characteristics. The annual-maxima series approach used in their threshold exceedance frequency calculation is biased low for frequent events (Karim et al., 2017; Pan et al., 2022), events that we suspect drive the bulk of in-channel geomorphic and ecological processes. The partial-duration series approach, on the other hand, could perform better on shorter record lengths (such as those available from high-frequency timeseries or for applications where only the recent hydroclimatic regime should be characterized) and could be applied on a seasonal basis (Armstrong et al., 2012; Karim et al., 2017; Pan et al., 2022). With only two studies on the conditional distribution of durations over a threshold, further exploration of the statistical distributions used by Correia and Feng et al. would be beneficial. Finally, the regression used to predict conditional distribution parameters as a function of threshold discharge should be validated at more riverine sites than the two examined in Feng et al. (2017).

This paper codifies the Duration-Over-Threshold model, a hierarchical statistical model inspired by Feng et al. (2017) that characterizes the return period of a given flowrate threshold being exceeded for a given duration. The objectives of this study are to 1) tailor the model of Feng et al. to frequent events (average recurrence less than 10 years) that we expect drive the bulk of geomorphological and ecohydrological processes (Karim et al., 2017); 2) refine and validate the structure of this model by fitting it at 33 stream gages

across the US state of Vermont; 3) relate the model parameters to catchment and reach physiographic characteristics, so that a regional model may be developed for use in ungauged hydrology; 4) present novel functional traits that summarize flood duration dynamics of a river's flow regime; and 5) provide tractable equations and computer software to enable the use of this model by river practitioners. In this process we hope to answer the following research questions:

- What is the relationship between threshold discharge and duration above that discharge for stream gages in Vermont?
- What is the best statistical distribution to represent flood duration over a threshold?
- What aspects of river flow regime are reflected within the model parameters?
- Which catchment and reach physiographic characteristics best predict model parameters, and can they tell us anything about some physical processes underlying the flow regime?

In Section 2.2, we introduce the model structure and necessary equations for its application (Section 2.2.1), describe the target study area of Vermont and how the model may be fit to streamflow data (Section 2.2.2), and document the steps we took to regionalize the model (Section 2.2.3). Section 2.3 demonstrates the model's competency at predicting frequency of low-magnitude events and characterizing flood durations (Section 2.3.1). Section 2.3.1 closes by describing novel watershed functional traits and briefly summarizing some scaling patterns. In Section 2.3.2, we present the results of the regionalization analysis, which enable the application of this model in ungauged catchments.

2.2 Methods

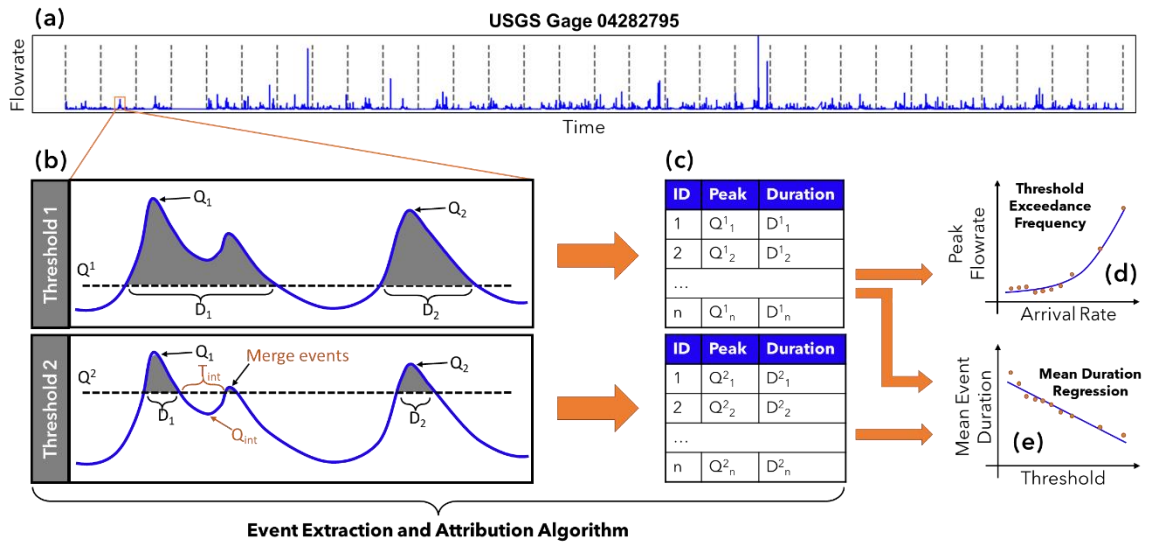


Figure 2-1. Graphical summary of flood event extraction and attribution algorithm at a single United States Geological Survey (USGS) gage. For a portion of the flowrate record of an example gage (USGS Stn 04282795), two example thresholds are shown along with their associated flood events (b, grey shading) and peak and duration characteristics (c). A dataset of flood characteristics at many thresholds may be used to fit the Duration-Over-Threshold model to generate a Threshold Exceedance Frequency relationship (d) and Mean Duration Regression (e).

2.2.1 Model Formulation

The Duration-Over-Threshold model defines a flood event as that portion of the hydrograph between the up-crossing and down-crossing limbs of a given flowrate threshold (each grey area, Figure 2-1b). By examining the series of flood events generated from a single flowrate threshold, the Peaks-Over-Threshold (POT) model can be used to develop a relationship between flowrate and the frequency with which it is exceeded (Figure 2-1d). Flood events from multiple flowrate thresholds can be used to generalize the relationship between threshold flowrate and the resulting population of flood durations (Figure 2-1e) in the style of Feng et al. (2017). These two model components can be combined to estimate

the return period associated with some flowrate threshold, q , being exceeded for some duration, d .

The threshold used to generate the POT series adds a degree of flexibility (and subjectivity) to POT analyses, and a consensus on the optimal method to select a threshold has not been established within the hydrologic literature (Lang et al., 1999; Pan et al., 2022). Two common approaches to threshold suitability determination (for models using the Generalized Pareto distribution) are the use of mean-excess plots and threshold stability plots, which have been well documented in Coles (2001). As noted by Coles, however, interpretation of linear/flat zones is highly subjective. For this analysis, we selected the threshold that yielded mean arrival rate of 4 events per year for the POT threshold. This is a relatively low threshold for FFA and was selected to better characterize the frequency distribution of more frequent events. The suitability of the resulting threshold was verified using mean-excess, threshold stability plots, and exponential arrival Quantile-Quantile (QQ) plots.

Once a POT series was generated, a statistical distribution was used to define the cumulative distribution function (CDF) of flood peaks, $F(q)$. The Poisson-Pareto POT model was used here because it is widely documented, has useful threshold suitability determination methods, and has a convenient closed form of the Generalized Extreme Value (GEV) distribution (Coles, 2001; Stedinger & Foufoula-Georgiou, 1993). The method of L-moments was used to estimate the Generalized Pareto Distribution (GPD) parameters because it is a deterministic method – as opposed to maximum-likelihood estimation – and can provide better parameter estimation for the highly skewed datasets

that are common in hydrology (Stedinger & Foufoula-Georgiou, 1993). GPD fit was assessed visually. We assumed a Poisson arrival process for flood peaks and fit an exponential distribution using a rate parameter, λ_b , equal to the number of peaks divided by the years of record.

This process was applied to multiple river gages (see Section 2.2.2). For each river gages and each threshold, we examined the goodness-of-fit of five probability distributions on the event duration series. We selected Pareto, gamma, exponential, two-parameter exponential, and GPD distributions for analysis because they are highly skewed distributions bounded on $(0, \infty)$. We used visual inspection and statistical tests to assess the goodness of fit at each gage and each flowrate threshold, and used these metrics to select the final distribution, $\mathbf{G}(\mathbf{d}|\mathbf{q})$, for use in the model.

To allow for the estimation of duration at flowrates between the analyzed thresholds, the relationship between flowrate and duration distribution must be generalized. Feng et al. (2017) proposed a relationship between stage and mean exceedance duration that was complex, involving four model coefficients. The regression was capable of modeling both tidal and riverine settings; but for riverine settings, the relationship reduced to an exponential decay function (i.e., $\mu = a \cdot \exp(b \cdot z)$). We performed an exploratory data analysis plotting various transformations of event durations, mean event durations, and median event durations versus event threshold. After observing a good visual fit between mean event duration and event threshold in double-log space, we compared a power law relationship ($\mu = Aq^B$) to the exponential decay relationship ($\mu = AB^q$) of Feng et al. (2017). We fit exponential decay functions and power law functions to the series of

threshold flowrate and mean event duration using the method of least squares. We then calculated the root mean squared log error (RMSLE) statistic for each of the two methods. In the final model parameterization, a model smearing coefficient \hat{E} was applied to correct for bias introduced in the method of least squares estimation (Duan, 1983), although its effect is negligible.

By extending the hierarchical peaks-over-threshold model with another conditional distribution representing event duration, our model defines arrival rate as:

$$\lambda(q, d) = \lambda_b [1 - F(q)][1 - G(d|q)] \quad (1)$$

in which, $\lambda(q, d)$ is the arrival rate with which flowrate q is exceeded for duration d (in events per year); λ_b is the mean arrival rate with which some base threshold (truncation threshold) is exceeded (in events per year); $F(q)$ is the percentile of q from the distribution of flow peaks above the base threshold; and $G(d|q)$ is the percentile of duration d from the distribution of events that exceeded flowrate q . In simpler terms, $\lambda(q, d)$ equals the rate with which some base threshold is exceeded times the probability that a higher threshold q is also exceeded times the probability that the higher threshold is exceeded for at least duration d .

Assuming the Pareto-Poisson POT model and a power-law regression, equation 1 may be rewritten as,

$$\lambda(q, d) = \left[1 - k \left(\frac{x - \xi}{\alpha} \right) \right]^{1/k} e^{\frac{-d}{\hat{E}Aq^B}} \quad (2)$$

(full derivation in Section 2.5.1). Figure 2-2 shows the graphical relationship between threshold, exceedance duration, and frequency for an example United States Geological Survey (USGS) gage. Figure 2-2b shows isolines representing events with different characteristics but the same arrival rate. For example, it is an equally rare event for 6,400 cfs to be exceeded for 15 minutes as it is for 2,000 cfs to be exceeded for 1 day. Another utility of the Duration-Over-Threshold model is that an event with 15-minute duration will have an equivalent arrival rate to the base flood frequency estimate.

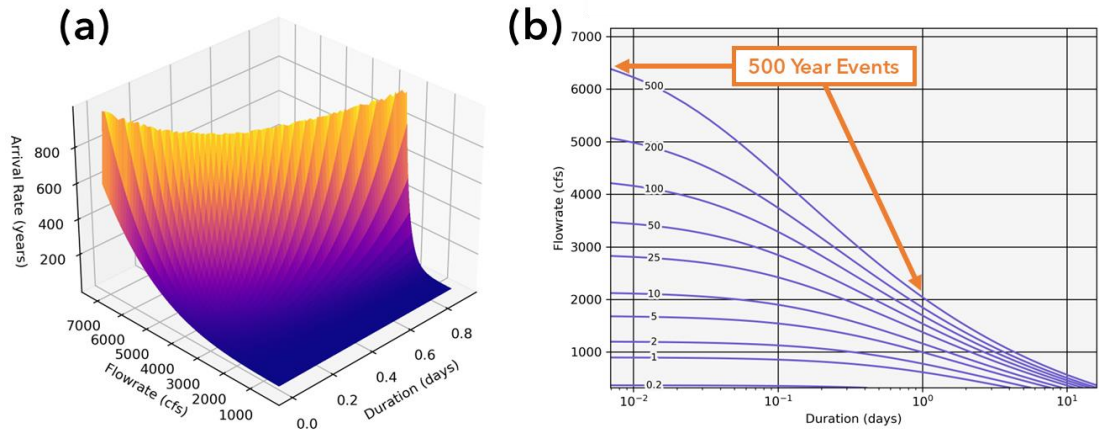


Figure 2-2 Fitted hierarchical model for flood frequency and duration at example gage 04282795. Blue lines in the right graphic represent isolines (events with different characteristics but the same recurrence interval).

It is also useful to calculate the duration from the threshold flowrate and recurrence interval,

$$d = -\hat{E}Aq^B * \ln \left[\lambda(q, d) * \left(1 - k \frac{q - \xi}{\alpha} \right)^{-1/k} \right] \quad (3)$$

or to work with Annual-Exceedance Probabilities.

$$AEP = 1 - \exp[-\lambda(q, d)] \quad (4)$$

2.2.2 Streamflow Records and Data Processing

We examined the mountainous US state of Vermont (VT) as a case study for duration dynamics across heterogeneous catchments. The 7,100 miles of perennial streams within VT range in form from mountain gorges to boggy wetlands and traverse the most remote areas of the state to more populous urban centers (VTDEC, 2018). Morphologic diversity within this relatively homogeneous humid temperate climatic region allows for the extraction of scaling relationships across topography and elevation without strong interference from climate signals. Vermont has a strong annual freeze-thaw cycle and high enough mountains to develop a snowpack. As a result, the largest volumes of water are passed through rivers during the winter and spring months (Scott et al., 2019). For Vermont rivers, streamflow data were obtained from USGS gaging stations. Of the 71 USGS stream gages listed within the state, a subset of 33 stations was selected based on their having more than 30 years of 15-minute instantaneous flowrate record (Figure 2-3 and Table 2-1).

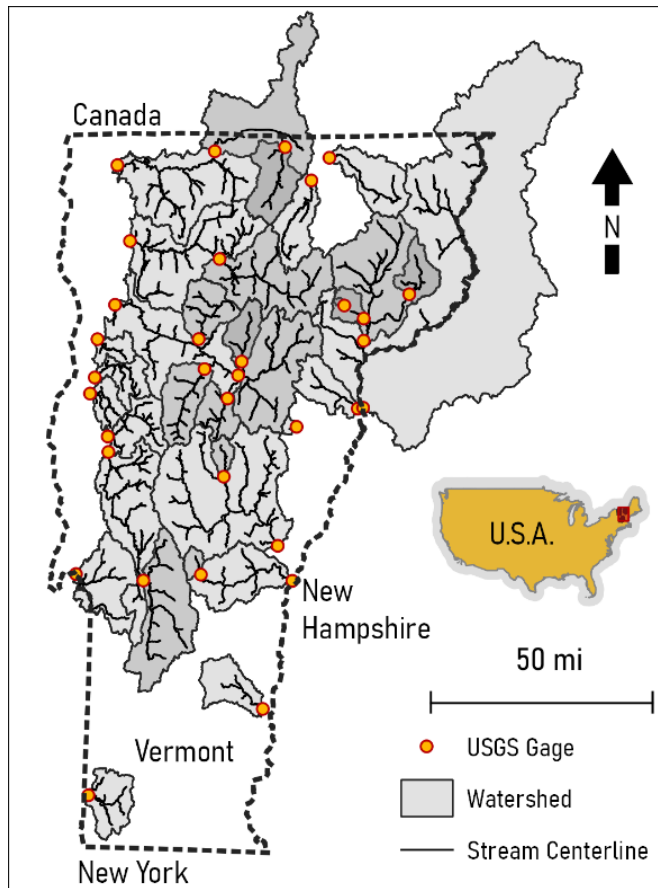


Figure 2-3 USGS gages within the state of Vermont having more than 30 years of 15-minute flowrate record. Darker shaded watersheds indicate areas where gages are nested.

Table 2-1 Summary of General Basin Characteristics

	<i>Drainage Area (Sq.km.)</i>	<i>Gage Elevation (m)</i>	<i>Basin Storage (%)</i>	<i>Average Yearly Precipitation (mm)</i>	<i>Analyzed Record Length (years)</i>
Minimum	8	30	0	970	31
Maximum	6,870	360	11	1,420	34
Average	820	150	3	1,200	32 (rounded)

From the 33 gages, we downloaded all complete water years of instantaneous (15-minute) and daily-averaged discharge record available as of January 1st, 2023 from the National Water Information System. Instantaneous flowrate records in our study area were prone to missing data that could potentially skew model fit. We filled data gaps for 25% of the data using a combination of forward-filling (5%) and daily-averaged discharge scaling (20%) (as described in Section 2.5.2) for model fitting.

To generate event populations at each flowrate threshold, we coded an algorithm that takes a flowrate timeseries and extracts flood events above a user-defined threshold, merges select events to ensure independence, and attributes each event with hydrologic event characteristics (Figure 2-1b). Although a great number of characteristics could be recorded, for this analysis we chose to attribute each event with three characteristics: 1) duration, defined as the time between up-crossing and down-crossing hydrograph limbs, 2) peak flowrate, defined as the maximum flowrate within the event, and 3) base threshold, defined as the threshold that generated the event.

We ran the algorithm at 30 thresholds per gage, which maximizes accuracy in the mean event duration regression and minimizes computational/data storage burdens. The lowest threshold was set at the flowrate that yielded the maximum number of cleaned events. The highest threshold was set as the highest flowrate to generate three independent flood events. The remaining 28 thresholds were evenly spaced between the maximum and minimum.

To ensure event independence, we included both minimum interevent duration and minimum recession enforcement within the algorithm. We defined independent flood

peaks to have both 1) at least five days of separation, plus the natural logarithm of the selected basin area and 2) a minimum interevent flowrate of at most 0.75 times the lower of the two adjacent peaks (Pan et al., 2022). Events not meeting these criteria were merged along with the interevent period between them.

2.2.3 Model Regionalization

To enable the estimation of flow regime at ungauged locations within Vermont and explore which watershed traits influence the duration component of flow regime, we performed a regional regression analysis. We fit multiple linear regressions that allow prediction of the five fitted parameters of the Duration-Over-Threshold model (ξ, α, k, A, B) from catchment- and reach-scale physiographic attributes. Our dataset of 92 physiographic characteristics was sourced from the USGS GAGES-II dataset (Falcone, 2011) and a GIS analysis using HEC-HMS and QGIS. We selected 66 attributes from the GAGES-II dataset that we believed would be potentially relevant to flood frequency and flood duration. To access more attributes related to catchment shape and channel slopes, we conducted a GIS analysis using the Hydrologic Engineering Center Hydrologic Modeling System (HEC-HMS) and QGIS. Several derived variables were also added to the dataset. GIS and transformation details are fully described in Section 2.5.3 along with the full list of 92 characteristics.

To balance input data requirements and predictive ability of the regional regression, we elected to use a maximum of three predictors for each of our model parameters. Linear regression coefficients were estimated using Ordinary Least Squares (OLS). While Generalized Least Squares (GLS) is generally preferred for regional hydrologic analyses

(Olson, 2014; Tasker & Stedinger, 1989), we had no reasonable basis to define a covariance matrix for this regression, and elected to use OLS instead. To find the best combination of three predictors, we compared regression R-Squared values from all combinations of three predictors. For each of the five model parameters, this amounted to 125,580 regressions.

2.3 Results & Discussion

2.3.1 Model Performance

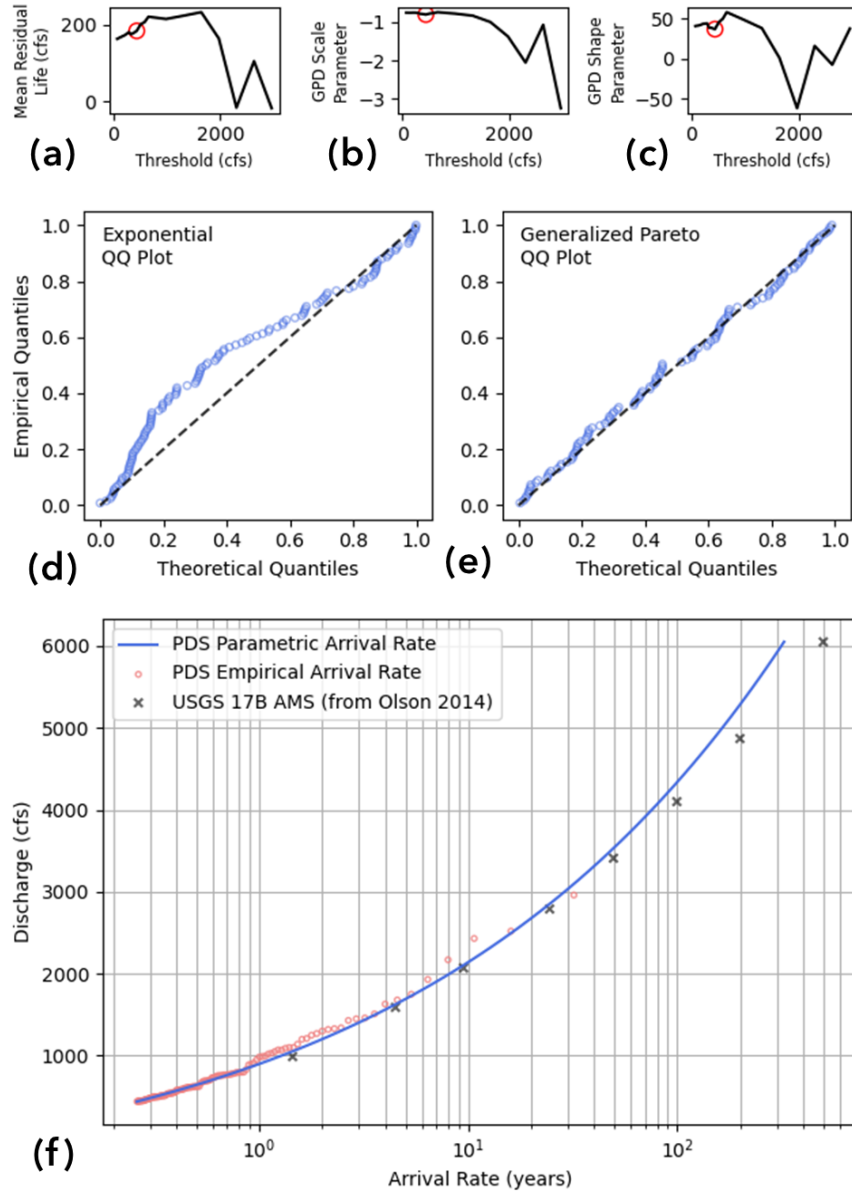


Figure 2-4 Fitting of the marginal distribution for example gage 04282795. (a-c) diagnostic plots after Coles (2001) illustrate the position of the select POT threshold (red circle); (d) QQ plots of observed interevent durations fitted to an exponential distribution; (e) observed flood peaks fitted to a Generalized Pareto distribution. (f) threshold exceedance frequency relationship with plotting positions of the peaks that generated it (red circled) and reference recurrence intervals from an annual-maxima (AM) USGS 17B analysis (Olson, 2014). Note that the AM recurrence intervals were converted to arrival rate using the equation $\text{Arrival Rate (years)} = -\ln(1 - \text{AEP}\%)$.

Results from our POT modeling show that our threshold exceedance frequency relationships represent the frequency of events with arrival rate less than ten years very well. We found interpretation of the Mean-excess and threshold stability plots (Figure 2-4a-c) to be too subjective to determine threshold suitability. Graphical assessment of the QQ plots (Figure 2-4d-e) and arrival rate plots (Figure 2-4f), however, showed good agreement between the empirical distribution of flood peaks and the fitted parametric estimation of flood peaks (POT model) at all gages. The POT model matched the flood peak plotting positions better than the quantiles from the Olson (2014) annual-maxima (AM) analysis, indicating a better characterization of flood frequency for events with recurrence interval less than 10 years. Unlike the AM approach, our threshold exceedance frequency relationship is also able to model flowrates with arrival rate less than one year. While modeling floods with sub-annual frequency is useful for many geomorphic and ecohydrologic applications, a proper characterization of the frequency of low magnitude floods also improves the model's ability to characterize infrequent, long duration floods at these low flowrates.

Our model matched the POT series better than Olson, and while POT and AMS estimates should converge after a recurrence interval of about 10 years, some gages did not. While it's impossible to determine the "correct" frequency for these rarer events, the discrepancy may come from three sources. First, we elected to choose a low truncation threshold for the PDS (4 events per year). This was intentional to weight the frequent events more heavily, but it may have decreased the model fit to rarer events. Second, the two analyses used different statistical distributions (curve shape) and parameter estimation

methods. Third, Olson had access to longer records of annual maxima than our thirty years of flow record, which could lead to a better characterization in the tail of the frequency distribution.

(NB: Plots in the style of Figure 2-4 were prepared on a gage by gage basis, and are available on CUAHSI Hydroshare)

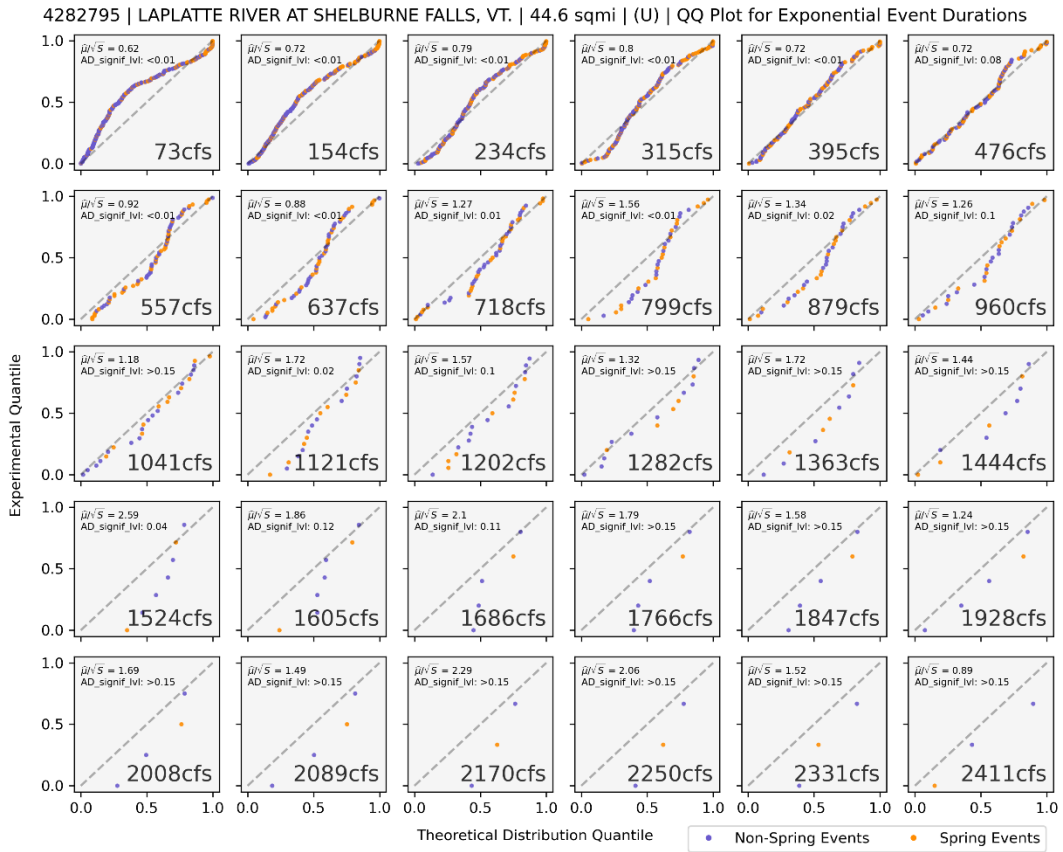


Figure 2-5 QQ plots of event duration empirical percentiles vs fitted exponential distribution percentiles at 30 discharge thresholds for example gage 04282795. The ratio of mean to variance is reported in the top left of each plot and should equal one for the exponential distribution. Anderson Darling test statistics are reported along with their 0.05 significance level values.

Visual comparison using five candidate distributions of event duration showed the exponential distribution to be satisfactory for the Duration-Over-Threshold model. Visual inspection was carried out by examining plots in the style of Figure 2-5. Fitting the Pareto distribution using the method of moments yielded distributions that were skewed low compared to the data and had very poor fit. The gamma distribution, also fit using the method of moments, showed reasonable performance for moderate and high thresholds, but did not capture the upper tail of the observed durations on the lower thresholds. While the exponential distribution generally fit the observed data well, it had a noticeable improvement in fit with increasing threshold. The two-parameter exponential distribution was fit using the method of L-moments, and although it had very good performance in the upper thresholds, it performed poorly on lower thresholds and exhibited some instability. The GPD distribution using L-moments had the best fit and showed solid performance at all thresholds. However, as a three-parameter distribution, developing a parameterization scheme as a function of flowrate would be challenging. The exponential distribution, in contrast, uses a single parameter and offered acceptable performance.

The poor fit of the exponential distribution at lower thresholds may be reflecting a mixed population of both rainfall floods and spring melt floods. Most high-duration low-threshold events within our dataset occurred between February and May, when spring thaw is common in Vermont (orange dots in Figure 2-5 top panel). Building separate spring and summer/fall Duration-Over-Threshold models would likely yield reasonable exponential distribution fits at all thresholds. Similarly, the exponential distribution should yield better fits at low thresholds in regions without strong spring thaw effects. The effect of treating

the mixed population as a single population, as we have done in this analysis, will be a systemic bias towards predicting longer durations than reality at low thresholds.

(NB: Plots in the style of Figure 2-5 were prepared on a gage by gage basis, and are available on CUAHSI Hydroshare)

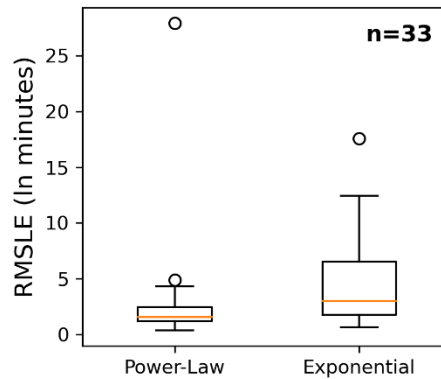


Figure 2-6 Comparison of RMSE evaluation metrics for Power Law and exponential decay functions to summarize the Mean Event Duration Relationship

For riverine gages, the relationship between event threshold and mean event duration follows a power law relationship. Power law and exponential decay regressions had average RMSLE values of 2.7 and 4.9, respectively, across our 33 study gages (Figure 2-6). Performance was not just better on average but excelled at most gages, and the power law regression had a lower RMSLE value than the exponential decay at 31 of 33 gages. The proposed power-law relationship is different than the exponential relationship proposed by Feng et al. (2017) and represents a significant improvement of the Duration-Over-Threshold model over their model for riverine sites.

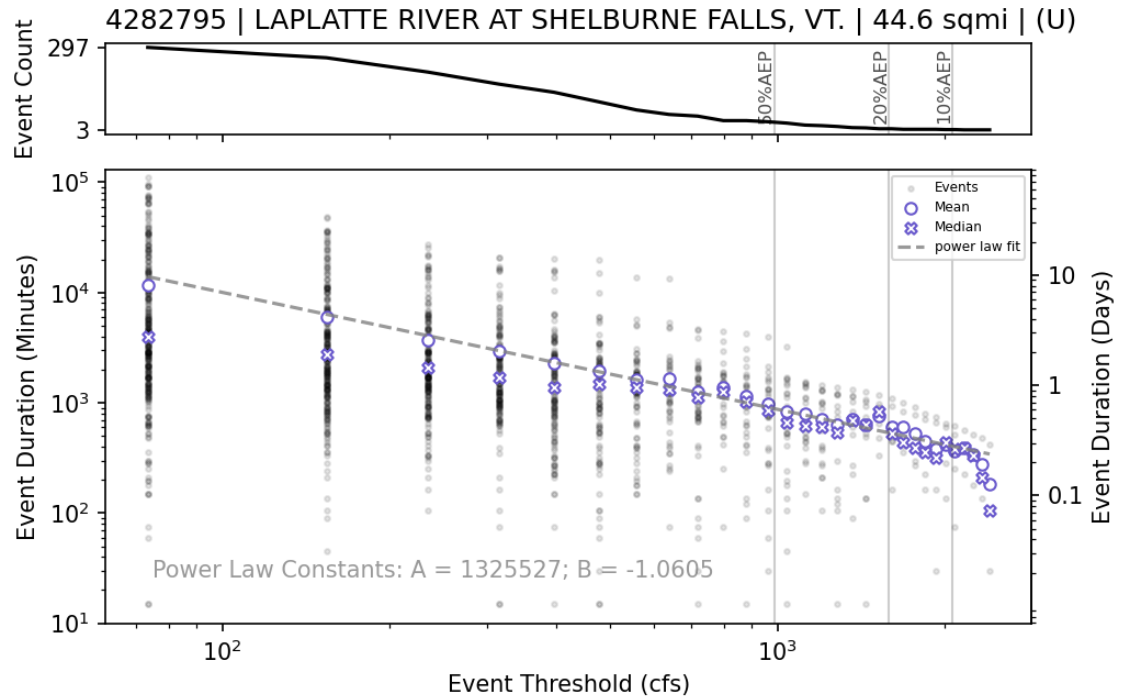


Figure 2-7 Fitting of the power law regression at example gage 04282795. Upper panel: the frequency of events by event threshold with recurrence intervals from Olson (2014). Lower panel: a power law fit to the mean of event duration by event threshold, with constants of slope (B) and intercept (A).

Beyond providing a better fit to the observed data, we suggest that the intercept and slope parameters of the power law regression (A, B) may be used as functional traits of river flow regime. Specifically, we interpret the A parameter as broadly representing mean event duration. This metric can be used to generally compare whether events along one river tend to persist longer than events along another river. We interpret the B parameter as representing the slope of the hydrograph between base and peak. More negative B values represent hydrographs that peak and then immediately recede while less negative B values represent hydrographs that peak and tend to stay high for longer durations.

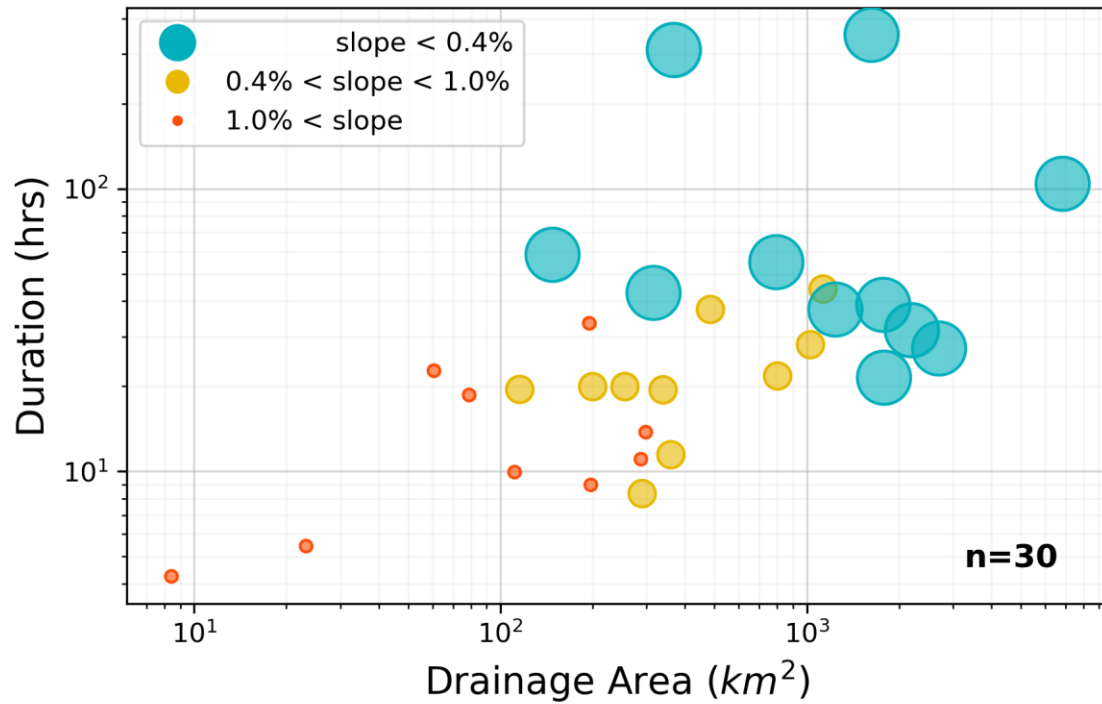


Figure 2-8 Duration of the 10-year exceedance of bankfull depth versus drainage area. Bankfull depth is defined as the depth exceeded every two years. Point color and size reflect the slope (in m/m) of the 10-85 flowpath (details in Section 2.5.3).

More tangible metrics may also be extracted from the Duration-Over-Threshold model to reflect river flow regime and yield insight into hydrologic processes. Figure 2-8 offers a simple example of how the model may be used to compare hydrologic characteristics across a region. The Figure shows the 10-year duration of bankfull depth exceedance for the study area (bankfull here defined as the 2-year event). This relationship could serve as a rule of thumb for river scientists within the region, a performance envelope for modelers to calibrate physical model to (as suggested by Hrachowitz et al. (2013)), or could be compared to other regions to assess the influence of climate on flood duration. Other plots of this style could be used within a comparative hydrology workflow (e.g. Gaál

et al. (2012)) or within a functional trait framework (Diehl et al., 2017; Funk et al., 2017) to relate flood duration to causal and effective watershed processes.

(NB: Plots in the style of Figure 2-7 were prepared on a gage by gage basis, and are available on CUAHSI Hydroshare)

2.3.2 Model Regionalization

The five model parameters estimated for each of the 33 gages are shown in Table 2-2. Some gages are located directly downstream of large dams, and the flow regulation from those structures caused flat threshold-duration relationships at 01151500, 04285500 and an increasing relationship at 04289000. Given the poor power law fits, these gages were not used in the regional regression. An additional four gages (01138500, 04293000, 04293500, and 04294000) were absent from the GAGES-II dataset and were not used in the regional regression. The remaining 26 gages were used along with the 92 physiographic characteristics to generate regional regressions for the Duration-Over-Threshold model parameters. A ranking of the 10 best regression models for each Duration-Over-Threshold parameter is shown in Table 2-3.

Table 2-2 Duration-Over-Threshold Model Parameters fit at 33 USGS gages within the US state of Vermont.

USGS Site No.	ξ	α	k	A (minutes)	B (min/cfs)	E
01134500	1845	723	0.1	8.52E+06	-1.14	1.02
01135150	142	57	-0.2	3.48E+05	-1.48	1.02
01135300	1469	703	-0.4	5.90E+05	-0.97	1.04
01135500	6823	2429	-0.1	5.12E+08	-1.40	1.05
01138500**	25606	8964	0.0	1.36E+10	-1.46	1.06
01139000	1681	635	-0.1	1.39E+08	-1.59	1.03
01139800	268	107	-0.2	9.34E+06	-1.85	1.07
01142500	728	340	-0.4	1.33E+07	-1.43	1.02
01144000	15471	6287	-0.1	1.92E+09	-1.49	1.02
01150900	843	301	0.0	2.55E+06	-1.14	1.08
01151500*	3807	606	0.5	1.56E+07	-1.09	1.04
01153550	4525	1852	-0.1	2.13E+07	-1.28	1.02
01334000	3004	1174	-0.1	1.34E+08	-1.54	1.04
04280000	2644	1175	-0.3	2.85E+07	-1.22	1.02
04282000	3972	1553	-0.1	4.22E+09	-1.71	1.02
04282500	3082	1628	0.4	5.07E+09	-1.56	1.07
04282525	3825	1639	-0.4	1.44E+06	-0.93	1.03
04282650	695	272	-0.1	1.03E+06	-0.91	1.02
04282780	1521	685	-0.2	1.28E+07	-1.28	1.01
04282795	899	400	-0.2	1.33E+06	-1.06	1.01
04285500*	935	90	0.4	9.19E+03	-0.06	1.02
04286000	5408	1756	0.0	8.92E+09	-1.82	1.05
04287000	2755	1351	-0.3	4.34E+07	-1.43	1.01
04288000	5145	1826	-0.2	1.12E+07	-1.16	1.03
04289000*	1438	542	-0.3	1.23E+07	-1.17	1.45
04290500	19132	5418	0.3	4.16E+09	-1.52	1.02
04292000	6885	2341	0.0	1.22E+08	-1.32	1.02
04292500	11986	4119	-0.1	4.32E+08	-1.31	1.01
04293000**	4819	1789	-0.1	5.54E+06	-1.03	1.02
04293500**	9732	3282	0.0	3.74E+08	-1.33	1.03
04294000**	17101	5663	-0.1	1.51E+08	-1.19	1.04
04296000	1847	703	-0.1	3.99E+07	-1.31	1.03
04296500	814	605	-0.2	2.70E+07	-1.09	1.02
* Gage with severe flow regulation						
** Gage lacking physiographic characteristics						

The final set of regional regression equations is:

$$\ln(\xi) = 3.74 + 0.414S + 1.10DA - 0.205W \quad (5)$$

$$\ln(\alpha) = 2.96 + 0.360S + 1.02DA - 0.115W \quad (6)$$

$$k = -0.221 + 0.000169e^{DA} \quad (7)$$

$$\ln(A) = 2.42 + 1.80DA - 0.0838HGC + 2.45WD \quad (8)$$

$$B = -0.330 + 0.0443S + 0.0154HGC - 0.420WD \quad (9)$$

Where S is the natural logarithm of the 10-85 flowpath slope in ft/ft; DA is the natural logarithm of the drainage area in square kilometers; W is the percentage of the watershed classified as open water in the NLCD 2006 dataset; HGC is the percentage of soils in HGC; and WD is the average depth to the seasonally high water table in feet.

The top performing regressions for the flow frequency distribution location and scale parameters, ξ and α , included characteristics relating to basin size, mainstem/basin slope, and basin storage, which are amongst the most commonly used physiographic characteristics for regional hydrologic frequency analysis (Dawdy et al., 2012). To lessen the input data requirements without sacrificing predictive ability, the same three predictors were selected for the final regressions for ξ and α shown in equations 5 and 6.

USGS Bulletin 17B methods detail the commonly accepted practice for developing a regional skew coefficient (IACWD, 1982). According to the bulletin, distribution skew is highly sensitive to extreme events and benefits substantially from space-for-time substitutions. The preferred method for regionalization is the use of a skew isoline map; but after plotting a map of our frequency distribution shape parameter, k , we

could not trace any reasonable skew isolines (Supplementary Information 2.5.4). The second method suggested by 17B for skew regionalization is a regression equation. Unfortunately, the regression for our skew coefficient was poor, and as shown in Table 2-3, only achieved an R-Squared of 0.585. It's unclear whether poor performance stems from over-sensitivity in the fitting of k (as suggested by 17B), a lack of appropriate explanatory physiographic characteristics, basin heterogeneity across the state of Vermont, or too small a sample size (Bulletin 17B recommends using at least 40 stations to regionalize skew). The final Bulletin 17B generalized skew method uses the average station skew across all stations. To balance predictive regression predictive capacity and input data requirements, we proposed the drainage-area-only regression on k shown in equation 7 that yielded an R-squared value of 0.402 and had a better Root Mean Square Error value than assuming an average skew.

The best predictors for the power law constants corroborate the findings of Gaál et al. (2012) for factors that influence flood duration behavior over decadal scales. Gaál et al. (2012) found that while storm type and season affected flood duration of specific events, the long term behavior of a catchment was influenced most by slope, geology, and soil permeability. We noted that lumping floods from mixed generation processes (snowmelt, precipitation, etc) did have an impact on the fit of our model, which suggests that the event type does influence flood duration. When averaging event durations across decadal timescales, Gaál et al. (2012) found that slope, geology, and soil permeability will affect the flood durations from a given catchment, and many of our top performing regressions for power law constants were related to flowpath slope, baseflow/groundwater interaction

(BFI_AVE and WTDEPAVE), and soil permeability (HGC). The partitioning of rain and meltwater between surface and subsurface flow is largely a function of soil permeability, and the rapidity with which any subsurface flow reaches an adjacent channel is a function of the underlying geology (Dunne, 1978). Slope acts to modulate the speed of both overland and subsurface transit times, which in turn, influences typical flood durations.

Our analysis found catchment size to be one of the best predictors for the power law A constant, while the only impact of drainage area on event duration that Gaál et al. (2012) found was that while small catchments could have short and long duration events, large catchments tended to only have long duration events. In theory, the longer times of concentration typically found in larger catchments should lead to longer flood durations (Chow et al., 1988). Another likely explanation is that short duration (~1-10 hour), convective storm systems (typical size 5-50 km²) can produce a flood in a smaller catchment while their influence on flowrates in a larger catchment would be small. Larger (2,000-10,000 km²) synoptic-scale storms typically last longer (days) and can produce floods in both small catchments and large catchments (Hirschboeck et al., 2000).

Although the performance of the power law regionalization is satisfactory for engineering and river management applications in ungauged basins, further analyses could be completed to fine-tune the performance and explore duration processes. Soil was significant for determining the power law A and B coefficients, but GAGES-II derives these estimates from the coarse STATSGO dataset. Newer and higher resolution soils datasets exist and could be leveraged (Soil Survey Staff, 2023). Furthermore, none of the analyzed physiographic characteristics reflected the structure of the channel network in the

catchment, which likely plays a significant role in determining flood duration (Beven & Wood, 1993). Finally, the analysis presented above may be highlighting predictors that have linear relationships but ignoring important predictors with nonlinear impacts, or those factors that have strong interactions (e.g., Boolean presence of a major dam in the catchment or synergistic effect of soil type and soil thickness). A better analysis should leverage machine learning methods optimized to reveal nonlinear processes.

Table 2-3 Top performing regressions for each of the Duration-Over-Threshold model parameters. The subset of 10 regressions had the highest R-Squared values of the 125,580 regressions analyzed for each parameter.

Model Rank	Parameter 1	Parameter 2	Parameter 3	R-Squared
Log(ξ)				
1	wbody_index	log_DRAIN_SQKM	log_10-85 flowpath slope (FT/FT)	0.940
2	WATERNLCD06	log_DRAIN_SQKM	log_10-85 flowpath slope (FT/FT)	0.940
3	log_DRAIN_SQKM	log_10-85 flowpath slope (FT/FT)	log_HIRES_LENTIC_MEANSIZ	0.940
4	HIRES_LENTIC_PCT	log_DRAIN_SQKM	log_10-85 flowpath slope (FT/FT)	0.939
5	HIRES_LENTIC_MEANSIZ	log_DRAIN_SQKM	log_10-85 flowpath slope (FT/FT)	0.939
6	WATERNLCD06	MAINS800_FOREST	log_DRAIN_SQKM	0.938
7	RIP800_11	log_DRAIN_SQKM	log_10-85 flowpath slope (FT/FT)	0.937
8	HIRES_LENTIC_MEANSIZ	MAINS800_FOREST	log_DRAIN_SQKM	0.937
9	log_DRAIN_SQKM	log_Relief Ratio	log_HIRES_LENTIC_MEANSIZ	0.935
10	HIRES_LENTIC_PCT	MAINS800_FOREST	log_DRAIN_SQKM	0.934
Log(α)				
1	RAW_AVG_DIS_ALL_MAJ_DAMS	log_DRAIN_SQKM	log_Relief Ratio	0.945
2	RAW_DIS_NEAREST_MAJ_DAM	log_DRAIN_SQKM	log_Relief Ratio	0.945
3	MAINS800_FOREST	ELEV_MIN_M_BASIN	log_DRAIN_SQKM	0.944
4	log_DRAIN_SQKM	log_10-85 flowpath slope (FT/FT)	log_HIRES_LENTIC_MEANSIZ	0.941
5	log_DRAIN_SQKM	log_10-85 flowpath slope (FT/FT)	log_HIRES_LENTIC_PCT	0.941
6	RAW_AVG_DIS_ALL_MAJ_DAMS	log_DRAIN_SQKM	log_10-85 flowpath slope (FT/FT)	0.941
7	RAW_DIS_NEAREST_MAJ_DAM	log_DRAIN_SQKM	log_10-85 flowpath slope (FT/FT)	0.941
8	log_DRAIN_SQKM	log_Relief Ratio	log_HIRES_LENTIC_MEANSIZ	0.939
9	log_DRAIN_SQKM	log_Relief Ratio	log_HIRES_LENTIC_PCT	0.937
10	dam_index	log_DRAIN_SQKM	log_10-85 flowpath slope (FT/FT)	0.936
k				
1	DRAIN_SQKM	RAW_AVG_DIS_ALLDAMS	ELEV_MIN_M_BASIN	0.585
2	DRAIN_SQKM	RAW_DIS_NEAREST_DAM	ELEV_MIN_M_BASIN	0.584
3	RAW_AVG_DIS_ALLDAMS	ELEV_MIN_M_BASIN	10-85 flowpath length (MI)	0.577
4	RAW_AVG_DIS_ALLDAMS	ELEV_MIN_M_BASIN	Longest flowpath length (MI)	0.577
5	DRAIN_SQKM	ELEV_MIN_M_BASIN	RRMEDIAN	0.577
6	RAW_DIS_NEAREST_DAM	ELEV_MIN_M_BASIN	10-85 flowpath length (MI)	0.576
7	RAW_DIS_NEAREST_DAM	ELEV_MIN_M_BASIN	Longest flowpath length (MI)	0.576
8	DRAIN_SQKM	ELEV_MIN_M_BASIN	RRMEAN	0.575
9	RAW_DIS_NEAREST_DAM	RAW_AVG_DIS_ALLDAMS	ELEV_MIN_M_BASIN	0.573
10	PRECIP_SEAS_IND	10-85 flowpath length (MI)	log_STREAMS_KM_SQ_KM	0.570
Log(A)				
1	WTDEPAVE	HGC	log_DRAIN_SQKM	0.820
2	STRAHLER_MAX	BFI_AVE	log_10-85 flowpath slope (FT/FT)	0.820
3	MAINS100_DEV	RIP100_PLANT	log_10-85 flowpath slope (FT/FT)	0.819
4	STRAHLER_MAX	FORESTNLCD06	MAINS800_FOREST	0.814
5	MAINS100_DEV	RIP800_PLANT	log_10-85 flowpath slope (FT/FT)	0.813
6	MAINS100_DEV	DAXSlope	log_Relief Ratio	0.811
7	HGC	HGD	log_DRAIN_SQKM	0.809
8	STRAHLER_MAX	MAINS100_DEV	DAXSlope	0.809
9	RIP100_DEV	DAXSlope	TWI	0.808
10	STRAHLER_MAX	MAINS800_FOREST	RIP800_FOREST	0.808
B				
1	WTDEPAVE	HGC	dam_index	0.696
2	STOR_NID_2009	WTDEPAVE	HGC	0.694
3	MAINS100_FOREST	WTDEPAVE	HGC	0.692
4	WTDEPAVE	HGC	log_Centroidal flowpath slope (ft/ft)	0.682
5	RIP800_DEV	WTDEPAVE	HGC	0.678
6	WTDEPAVE	HGC	TWI	0.675
7	RAW_AVG_DIS_ALLDAMS	WTDEPAVE	HGC	0.675
8	DEVNLCD06	WTDEPAVE	HGC	0.675
9	RAW_DIS_NEAREST_DAM	WTDEPAVE	HGC	0.674
10	STRAHLER_MAX	WTDEPAVE	HGC	0.670

2.4 Conclusions

We developed an extension to the Peaks-Over-Threshold modeling approach that relates the duration spent over a flowrate threshold to a recurrence interval. The Duration-Over-Threshold model is similar to that of Feng et al. (2017), but includes several notable changes. By using the partial duration series instead of the annual maxima, our approach was able to properly model the frequency of frequent floods that drive many geomorphic and ecohydrological processes. The Duration-Over-Threshold model used discharge instead of stage records, allowing for regionalization of the model parameters and comparison of flow regime parameters across gauges. Our model was fit on higher-fidelity 15-minute data, which allowed for a more accurate characterization of flow regime, especially in smaller, flashier basins. We used a power law relationship between threshold flow rate and mean event duration, which was shown to be a better predictor than an exponential decay relationship at 31 of 33 USGS river gages within the state of Vermont.

This work not only improved the characterization of river flow regime within the model but also extended its useability. Tractable equations, open-source code, and documentation for the Duration-Over-Threshold model will make it more easily adopted by river practitioners. Furthermore, we developed regional regression equations to link model parameters to catchment- and reach-scale attributes. The regression equations enable model application in ungauged locations. A preliminary analysis of functional traits provided by the model found that flood duration tends to increase with drainage area but decreases in high-gradient streams and basins with low permeability soils.

Several Duration-Over-Threshold improvements could be pursued in the future. Seasonal analyses may be completed to separate out spring thaw dynamics, which are overwhelming the duration dynamics at low threshold flowrates (and such seasonal analyses have been enabled by the switch to POT frequency). The coefficient estimation within the regional regression analysis could be switched from OLS to GLS if a suitable covariance matrix is identified. Higher fidelity soils and land-cover datasets will likely improve regression performance and aid in duration process inference. Finally, a larger sample size (both number of gages and length of record) could improve regionalization of the frequency skew coefficient.

Future efforts to extend the Duration-Over-Threshold model could involve deriving design flood hydrographs from the duration estimates. The data and parameters could be modified to model power-over-threshold or volume-over-threshold for geomorphic and detention structure modeling, respectively. If the threshold is set at some critical threshold for bed mobilization, toe scour, or bank erosion, and a damage function is constructed based on event duration, the frequency distribution may be used to estimate reach susceptibility to erosion. Stage-Duration relationships could be used for fluvial landform delineation or ecological gradient mapping. Lastly, comparative hydrology, functional trait, and machine-learning workflows can be used to link model parameters A and B (and other derived traits) to both causal and effective processes, revealing reproducible patterns in watershed function and deepening our understanding of watershed systems.

2.5 Supporting Information

2.5.1 Model Derivation

To derive the closed form of the Duration-Over-Threshold model, we begin with the model structure,

$$\lambda(q, d) = \lambda_b[1 - F(q)][1 - G(d|q)]$$

in which, $\lambda(q, d)$ is the average number of events per year in which flowrate q is exceeded for duration d ; λ_b is the number of events per year in which some base threshold (truncation threshold) is exceeded; $F(q)$ is the Cumulative Distribution Function (CDF) of a Peaks-Over-Threshold (POT) series at threshold b ; and $G(d|q)$ is the CDF of a duration over threshold series at duration, q .

Assuming the Poisson-Pareto Peaks-Over-Threshold model, we can simplify the threshold exceedance frequency $\lambda_b[1 - F(q)]$ as,

$$\lambda(q) = \lambda_b[1 - F(q)]$$

$$\lambda(q) = \lambda_b \left[1 - k \frac{q - b}{\alpha^*} \right]^{1/k}$$

$$\lambda(q) = \left[\lambda_b^k - \lambda_b^k k \frac{q - b}{\alpha^*} \right]^{1/k}$$

$$\lambda(q) = \left[1 + (\lambda_b^k - 1) - \lambda_b^k k \frac{q - b}{\alpha^*} \right]^{1/k}$$

$$\lambda(q) = \left[1 + \lambda_b^k (1 - \lambda_b^{-k}) - \lambda_b^k k \frac{q - b}{\alpha^*} \right]^{1/k}$$

$$\lambda(q) = \left[1 + \frac{k\alpha^* \lambda_b^k (1 - \lambda_b^{-k})}{k\alpha^*} - \lambda_b^k k \frac{q - b}{\alpha^*} \right]^{1/k}$$

$$\lambda(q) = \left[1 - k \left(-\frac{\alpha^* \lambda_b^k (1 - \lambda_b^{-k})}{k\alpha^*} + \lambda_b^k \frac{q - b}{\alpha^*} \right) \right]^{1/k}$$

$$\lambda(q) = \left[1 - k \left(\frac{q - b - \frac{\alpha^* (1 - \lambda_b^{-k})}{k}}{\alpha^* \lambda_b^{-k}} \right) \right]^{1/k}$$

$$\lambda(q) = \left[1 - k \left(\frac{q - \xi}{\alpha} \right) \right]^{1/k}$$

Where,

$$\xi = b - \frac{\alpha^* (1 - \lambda_b^{-k})}{k}$$

$$\alpha = \alpha^* \lambda_b^{-k}$$

b is the base threshold flowrate and Generalized Pareto Distribution (GPD) location parameter, α^* is the GPD scale parameter, and k is the GPD shape parameter.

To simplify the conditional distribution of event durations, $[1 - G(d|q)]$, we begin with a power law relating threshold flowrate to mean event duration.

$$\mu = Aq^B$$

Power laws are subject to transformation bias when they are fit using the Ordinary Least Squares (OLS) in log-log space. Thus, we use the smearing estimate of Duan (1983) for mean duration.

$$\mu = \hat{E}Aq^B$$

Where

$$\hat{E} = \frac{1}{n} \sum_{i=1}^n \exp(\ln(\mu_{obs}) - \ln(Aq^B))$$

Assuming the duration series is exponentially distributed, with rate parameter μ , the CDF of durations will be

$$G(d) = 1 - e^{-\frac{d}{\mu}}$$

Substituting the power law for exponential rate parameter,

$$G(d|q) = 1 - e^{-\frac{d}{\hat{E}Aq^B}}$$

And out conditional distribution of event durations, $[1 - G(d|q)]$, can be simplified

$$[1 - (1 - e^{-\frac{d}{\hat{E}Aq^B}})]$$

$$e^{-\frac{d}{\hat{E}Aq^B}}$$

Combining these model components, we arrive at the Poisson-Pareto-Power Duration-Over-Threshold model.

$$\lambda(q, d) = \left[1 - k \left(\frac{q - \xi}{\alpha} \right) \right]^{1/k} e^{\frac{-d}{\hat{E}Aq^B}}$$

This may be solved for duration,

$$\lambda(q, d) * \left(1 - k \frac{q - \xi}{\alpha} \right)^{-1/k} = e^{\frac{-d}{\hat{E}Aq^B}}$$

$$\ln \left[\lambda(q, d) * \left(1 - k \frac{q - \xi}{\alpha} \right)^{-1/k} \right] = \frac{-d}{\hat{E}Aq^B}$$

$$d = -\hat{E}Aq^B * \ln \left[\lambda(q, d) * \left(1 - k \frac{q - \xi}{\alpha} \right)^{-1/k} \right]$$

2.5.2 Missing Data Handling

Instantaneous (15-minute) flowrate records in our study area were prone to missing data that can potentially skew model fit. Short spans of missing data, which we defined as shorter than 24 hours in duration, occurred sporadically throughout the flowrate records. Large spans of missing data – which we defined as longer than 24 hours in duration – occurred in early record years and frequently in winter months, when ice interfered with gaging instruments. Large spans of missing data are problematic because they have the potential to exclude flood peaks from the dataset, and can lead to an underestimation of flood frequency, if a significant peak(s) is omitted. If a significant peak occurs during a short span, the records bordering the gap will be near enough to the peak that the gap will be less likely to impact flood frequency estimates. Short spans of missing data, however,

will cause errors in the event extraction and attribution algorithm described in Figure 1 and Section 2.2.2.

To combat errors associated with missing data, we imputed data in two approaches to create a continuous flow series across each period of record. For short spans, we took the last observed flowrate prior to the gap and forward filled that value into missing data entries. We term this dataset the *filled timeseries*. To fill the large spans of missing data, we used a linear regression that relied on the mean daily flowrate, which was consistently provided by USGS for those days with missing instantaneous (15-minute) records. We fit a linear regression to mean daily flowrate and maximum instantaneous daily flowrate at each gage using data from all days that had complete instantaneous and daily-averaged flowrate records. Regression intercepts were fixed to zero so that a 0 cfs mean daily flow would map to a 0 cfs peak daily flow. These regression coefficients were multiplied by the mean daily flowrate series for the entire period of record to create an estimated daily maximum flowrate series. On days missing instantaneous flowrate values, we imputed the estimated daily maximum flowrate across the entire day. The resulting dataset is referred to as the *imputed timeseries*.

The *filled timeseries* was used to fit the mean duration regression while the *imputed timeseries* was used to fit the threshold exceedance frequency relationship. By imputing a fixed value across all missing data days in the *imputed timeseries*, estimates of event duration from those would not be credible. Furthermore, there existed enough flood events in the *filled timeseries* to confidently fit a mean duration regression. For both these reasons, the mean duration regression was fit using only the *filled timeseries*. Since the threshold

exceedance frequency relationship was sensitive to missing peaks but insensitive to having block-filled days, the *imputed timeseries* was used in its fitting.

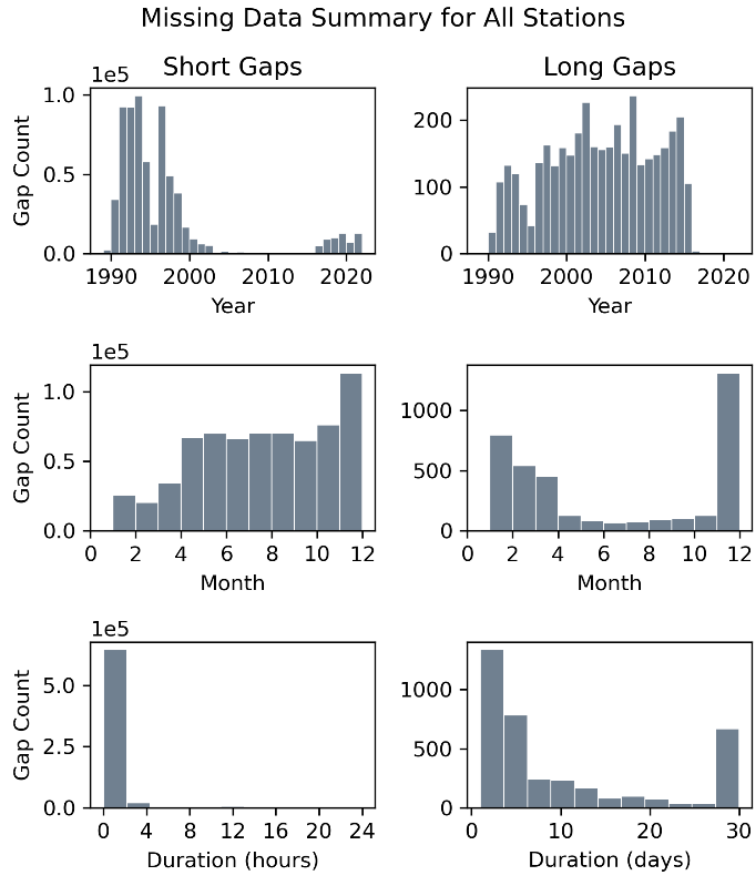


Figure 2-9 Description of time of occurrence as well as duration for short gaps (missing data periods with duration < 24 hours) and long gaps (missing data periods with duration > 24 hours). Long gap durations were truncated to 30 days for this histogram.

Short gaps in the instantaneous flowrate record, while commonplace, were insignificant in their duration. Figure 2-9 shows that short gaps occurred most frequently in the periods 1990-2000 and 2015-2022. This trend was consistent across all gages, but its source is unclear. Despite a clear temporal trend, we have no reason to suspect that filling data gaps in certain periods more than others will bias results. Figure 2-9 shows that many short gaps were shorter than two hours in duration. Given such short gaps in the

record, we expect that forward-filling adjacent flowrates is a reasonably accurate approach to predict flowrates within those gaps.

Long gaps in the instantaneous flowrate record occurred mostly in the winter months, when low flows tend to prevail in the Northeastern US (Scott et al., 2019). For all stations, long gaps are prevalent from 1990-2015. We suspect that in the mid 2010's the USGS changed their data cleaning process to estimate flows during record gaps. Long gaps show a clear seasonality, with almost all gaps occurring within the winter months (12, 1, 2, 3). This is likely due to the presence of river ice that can interfere with gage measurements. While most large gaps were less than 5 days in duration, there was a significant portion with duration greater than 30 days. For all the gages analyzed within this study, flood events could occur and recede within 24 hours, so any long gap has the potential to bias flood frequency estimates in the marginal distribution.

The linear regressions we developed between daily mean flow and daily peak flow at each station had good R-Squared values (maximum 0.99, minimum 0.59, and mean 0.89). Since many long gaps occurred in winter months and winter months typically contain lower flows for this region, the imputed value series contained entirely low to moderate flows for each gage. In fact, most of the imputed peak daily flow values did not exceed the event threshold used in the marginal frequency analysis.

2.5.3 Catchment and Reach Physiographic Characteristics

The 30m digital elevation models (DEMs) and stream centerlines were downloaded from the USGS National Map (USGS 2018, 2020). Stream centerlines were clipped to a 500m buffer around each USGS gage. The upstream elevation, downstream elevation, and

length of these centerlines were extracted in QGIS to derive the reach slope around each USGS gage (parameter **LocalSlope(m/m)**). Ten catchment characteristics were derived with HEC-HMS relating to catchment shape, mainstem slope, and mainstem length. Those characteristics were **Longest flowpath length (MI)**, **Longest flowpath slope (ft/ft)**, **Centroidal flowpath length (MI)**, **Centroidal flowpath slope (ft/ft)**, **10-85 flowpath length (MI)**, **10-85 flowpath slope (FT/FT)**, **Basin slope (FT/FT)**, **Basin relief (FT)**, **Relief Ratio**, and **Elongation Ratio**.

Several derived variables were also added to the dataset. The five basin characteristics were derived from multiplying and dividing GAGES-II attributes and GIS attributes (parameters **DAXSlope**, **TWI**, **dam_index**, **wbody_index**, and **spring_melt_index**). We visually inspected histograms for all 81 variables and selected any skewed histograms for logarithmic transformation. A total of 11 basin characteristics were logarithmically transformed. Both the original 11 and transformed 11 were retained in the final dataset. The final dataset is shown in Table 2-4.

Table 2-4 List of generated physiographic basin and reach characteristics.

Characteristic name	Description
DRAIN_SQKM	Watershed drainage area, sq km, as delineated in our basin boundary
BAS_COMPACTNESS	Watershed compactness ratio, = area/perimeter ² * 100; higher number = more compact shape.
PPTAVG_BASIN	Mean annual precipitation (cm) for the watershed, from 800m PRISM data. 30 years period of record 1971-2000.
PRECIP_SEAS_IND	Precipitation seasonality index (Markham, 1970; Dingman, 2002). Index of how much annual precipitation falls seasonally (high values) or spread out over the year (low values). Based on monthly precipitation values from 30 year (1971-2000) PRISM. Range is 0 (precipitation spread out exactly evenly in each month) to 1 (all precipitation falls in a single month).
STREAMS_KM_SQ_KM	Stream density, km of streams per watershed sq km, from NHD 100k streams
STRAHLER_MAX	Maximum Strahler stream order in watershed, from NHDPlus.
MAINSTEM_SINUOSITY	Sinuosity of mainstem stream line, from our delineation of mainstem stream lines (see Falcone and others, 2010b). Defined as curvilinear length of the mainstem stream line divided by the straight-line distance between the end points of the line.
HIRES_LENTIC_PCT	Percent of watershed surface area covered by "Lakes/Ponds" + "Reservoirs" in NHD Hi-Resolution (1:24k) data
BFI_AVE	Base Flow Index (BFI), The BFI is a ratio of base flow to total streamflow, expressed as a percentage and ranging from 0 to 100. Base flow is the sustained, slowly varying component of streamflow, usually attributed to ground-water discharge to a stream.
PERDUN	Dunne overland flow, also known as saturation overland flow, is generated in a basin when the water table "outcrops" on the land surface (due to the infiltration and redistribution of soil moisture within the basin), thereby producing temporary saturated areas. These saturated areas generate Dunne overland flow through exfiltration of shallow ground water and by routing precipitation directly to the stream network.
PERHOR	Horton overland flow, also known as infiltration-excess overland flow, is generated in a basin when infiltration rates are exceeded by precipitation rates.
TOPWET	Topographic wetness index, $\ln(a/S)$; where "ln" is the natural log, "a" is the upslope area per unit contour length and "S" is the slope at that point. See

	http://ks.water.usgs.gov/Kansas/pubs/reports/wrir.99-4242.html and Wolock and McCabe, 1995 for more detail.
CONTACT	Subsurface flow contact time index. The subsurface contact time index estimates the number of days that infiltrated water resides in the saturated subsurface zone of the basin before discharging into the stream.
RUNAVE7100	Estimated watershed annual runoff, mm/year, mean for the period 1971-2000. Estimation method integrated effects of climate, land use, water use, regulation, etc.
WB5100_MAR_MM	Estimated watershed March runoff, mm/month, mean for the period 1951-2000. From Wolock and McCabe (1999) water balance model. Estimates the effects of precipitation and temperature, but not other factors (land use, water use, regulation, etc.)
WB5100_APR_MM	Estimated watershed April runoff, mm/month, mean for the period 1951-2000. From Wolock and McCabe (1999) water balance model. Estimates the effects of precipitation and temperature, but not other factors (land use, water use, regulation, etc.)
PCT_1ST_ORDER	Percent of stream lengths in the watershed which are first-order streams (Strahler order); from NHDPlus
PCT_2ND_ORDER	Percent of stream lengths in the watershed which are second-order streams (Strahler order); from NHDPlus
PCT_3RD_ORDER	Percent of stream lengths in the watershed which are third-order streams (Strahler order); from NHDPlus
PCT_4TH_ORDER	Percent of stream lengths in the watershed which are fourth-order streams (Strahler order); from NHDPlus
PCT_5TH_ORDER	Percent of stream lengths in the watershed which are fifth-order streams (Strahler order); from NHDPlus
PCT_6TH_ORDER_OR_MORE	Percent of stream lengths in the watershed which are sixth or greater-order streams (Strahler order); from NHDPlus
STOR_NID_2009	Dam storage in watershed ("NID_STORAGE"); megaliters total storage per sq km (1 megaliters = 1,000,000 liters = 1,000 cubic meters). Also see note to the right.
STOR_NOR_2009	Dam storage in watershed ("NORMAL_STORAGE"); megaliters total storage per sq km (1 megaliters = 1,000,000 liters = 1,000 cubic meters)
RAW_DIS_NEAREST_DAM	Raw straightline distance (km) of gage location to nearest dam in watershed.
RAW_AVG_DIS_ALLDAMS	Raw average straightline distance (km) of gage location to all dams in watershed.
RAW_DIS_NEAREST_MAJ_DAM	Raw straightline distance (km) of gage location to nearest major dam in watershed.
RAW_AVG_DIS_ALL_MAJ_DAMS	Raw average straightline distance (km) of gage location to all major dams in watershed.

FRAGUN_BASIN	Fragmentation Index of "undeveloped" land in the watershed. High numbers = more disturbance by development and fragmentation; a very pristine basin with a lot of contiguous undeveloped land cover would have a low number
HIRES_LENTIC_MEANSIZ	Mean size (ha) of Lakes/Ponds + Reservoir water bodies from NHD Hi-Resolution (1:24k) data
DEVNLCD06	Watershed percent "developed" (urban), 2006 era (2001 for AK-HI-PR). Sum of classes 21, 22, 23, and 24
FORESTNLCD06	Watershed percent "forest", 2006 era (2001 for AK-HI-PR). Sum of classes 41, 42, and 43
PLANTNLCD06	Watershed percent "planted/cultivated" (agriculture), 2006 era (2001 for AK-HI-PR). Sum of classes 81 and 82
WATERNLCD06	Watershed percent Open Water (class 11)
MAINS100_DEV	Mainstem 100m buffer "developed" (urban), 2006 era. Sum of MAINS100_21, 22, 23, and 24. Buffer is the approximate area 100m each side of stream centerline
MAINS100_FOREST	Mainstem 100m buffer "forest", 2006 era. Sum of MAINS100_41, 42, and 43
MAINS100_PLANT	Mainstem 100m buffer "planted/cultivated" (agriculture), 2006 era. Sum of MAINS100_81 and 82
MAINS100_11	Mainstem 100m buffer percent Open Water
MAINS800_DEV	Mainstem 800m buffer "developed" (urban), 2006 era. Sum of MAINS800_21, 22, 23, and 24. Buffer is the approximate area 800m each side of stream centerline
MAINS800_FOREST	Mainstem 800m buffer "forest", 2006 era. Sum of MAINS800_41, 42, and 43
MAINS800_PLANT	Mainstem 800m buffer "planted/cultivated" (agriculture), 2006 era. Sum of MAINS800_81 and 82
MAINS800_11	Mainstem 800m buffer percent Open Water
RIP100_DEV	Riparian 100m buffer "developed" (urban), 2006 era. Sum of RIP100_21, 22, 23, and 24. Buffer is the approximate area 100m each side of stream centerline, for all streams in watershed
RIP100_FOREST	Riparian 100m buffer "forest", 2006 era. Sum of RIP100_41, 42, and 43
RIP100_PLANT	Riparian 100m buffer "planted/cultivated" (agriculture), 2006 era. Sum of RIP100_81 and 82
RIP100_11	Riparian 100m buffer percent Open Water
RIP800_DEV	Riparian 800m buffer "developed" (urban), 2006 era. Sum of RIP800_21, 22, 23, and 24. Buffer is the approximate area 800m each side of stream centerline, for all streams in watershed

RIP800_FOREST	Riparian 800m buffer "forest", 2006 era. Sum of RIP800_41, 42, and 43
RIP800_PLANT	Riparian 800m buffer "planted/cultivated" (agriculture), 2006 era. Sum of RIP800_81 and 82
RIP800_11	Riparian 800m buffer percent Open Water
PERMAVE	Average permeability (inches/hour)
WTDEPAVE	Average value of depth to seasonally high-water table (feet)
ROCKDEPAVE	Average value of total soil thickness examined (inches)
RFACT	Rainfall and Runoff factor ("R factor" of Universal Soil Loss Equation); average annual value for period 1971-2000
HGC	Percentage of soils in hydrologic group C. Hydrologic group C soils have slow soil infiltration rates. The soil profiles include layers impeding downward movement of water and, typically, have moderately fine or fine texture.
HGD	Percentage of soils in hydrologic group D. Hydrologic group D soils have very slow infiltration rates. Soils are clayey, have a high-water table, or have a shallow impervious layer.
HGCD	Percentage of soils in hydrologic group C/D. Hydrologic group C/D soils have group C characteristics (slow infiltration rates) when artificially drained and have group D characteristics (very slow infiltration rates) when not drained.
ELEV_MAX_M_BASIN	Maximum watershed elevation (meters) from 100m National Elevation Dataset
ELEV_MIN_M_BASIN	Minimum watershed elevation (meters) from 100m National Elevation Dataset (may include sinks)
ELEV_MEAN_M_BASIN	Mean watershed elevation (meters) from 100m National Elevation Dataset
ELEV_STD_M_BASIN	Standard deviation of elevation (meters) across the watershed from 100m National Elevation Dataset
RRMEAN	Dimensionless elevation - relief ratio, calculated as $(ELEV_MEAN - ELEV_MIN)/(ELEV_MAX - ELEV_MIN)$.
RRMEDIAN	Dimensionless elevation - relief ratio, calculated as $(ELEV_MEDIAN - ELEV_MIN)/(ELEV_MAX - ELEV_MIN)$.
SLOPE_PCT	Mean watershed slope, percent. Derived from 100m resolution National Elevation Dataset, so slope values may differ from those calculated from data of other resolutions.
ASPECT_DEGREES	Mean watershed aspect, degrees (degrees of the compass, 0-360). Derived from 100m resolution National Elevation Data. 0 and 360 point to north. Because of the national Albers projection actual aspect may vary.
Longest flowpath length (MI)	The longest flowpath extends from the subbasin outlet to the most hydraulically-remote point upstream. Longest flowpath is significant in that it is typically used to determine the time of concentration for a watershed.

Longest flowpath slope (ft/ft)	Slope of longest flowpath
Centroidal flowpath length (MI)	The centroidal flowpath is a subset of longest flowpath. It begins at the subbasin outlet and extends upstream along the longest flowpath until it reaches the point along the longest flowpath that is nearest to the subbasin centroid. A comparison of centroidal flowpath and longest flowpath can be seen in the image below.
Centroidal flowpath slope (ft/ft)	slope of centroidal flowpath
10-85 flowpath length (MI)	The 10-85 flowpath is also a subset of longest flowpath. Measuring from the outlet in the upstream direction, the 10-85 flowpath begins at a point representing ten percent of the total length of the longest flowpath and ends at a point representing eighty-five percent of the total length. Both the length and the slope of the 10-85 flowpath are provided in the subbasin statistics table, shown above. The 10-85 slope is often more representative of flowpath slopes as a whole within the watershed as it is not affected by the more extreme upstream elevations of the longest flowpath that are typically found near the watershed divide. A comparison of 10-85 flowpath and longest flowpath can be observed in the image below.
10-85 flowpath slope (FT/FT)	flope of 10-85 flowpath
Basin slope (FT/FT)	The basin slope represents the average slope of the entire subbasin (rise/run). For each elevation raster value within the subbasin, the algorithm scans the surrounding eight neighbors and computes the slope using the maximum scanned elevation difference. The algorithm does not weigh north, east, south, and west neighbors more than diagonal neighbors; each neighbor is considered equally. The basin slope output is the average of all the computed slope values in the subbasin.
Basin relief (FT)	Basin relief represents the elevation difference between the highest point on the drainage divide and the outlet point of the subbasin.
Relief Ratio	The relief ratio is simply the basin relief divided by the length of the longest flowpath.
Elongation Ratio	The elongation ratio is a dimensionless ratio used to categorize the general shape of a subbasin. It is a ratio between the diameter of a circle with the same area as the subbasin and the basin length. Elongation ratio values typically range from ~0.2 to 1.0, with lower values representing elongated basins and values close to 1 representing circular basins.
LocalSlope(m/m)	Slope of the reach within a 500-meter buffer of the gage.
DAXSlope	DRAIN_SQKM times by local slope

TWI	DRAIN_SQKM divided by local slope
dam_index	STOR_NID_2009 divided by RUNAVE7100
wbody_index	HIRES_LENTIC_PCT divided by RUNAVE7100
spring_melt_index	Average of WB5100_MAR_MM and WB5100_APR_MM divided by RUNAVE7100
log_power_a	Natural Logarithm of power_a
log_power_a_raw	Natural Logarithm of power_a_raw
log_xi	Natural Logarithm of xi
log_alpha	Natural Logarithm of alpha
log_DRAIN_SQKM	Natural Logarithm of DRAIN_SQKM
log_Relief Ratio	Natural Logarithm of Relief Ratio
log_Longest flowpath slope (ft/ft)	Natural Logarithm of Longest flowpath slope (ft/ft)
log_Centroidal flowpath slope (ft/ft)	Natural Logarithm of Centroidal flowpath slope (ft/ft)
log_10-85 flowpath slope (FT/FT)	Natural Logarithm of 10-85 flowpath slope (FT/FT)
log_DAxSlope	Natural Logarithm of DAxSlope
log_HIRES_LENTIC_PCT	Natural Logarithm of HIRES_LENTIC_PCT
log_HIRES_LENTIC_MEANSIZ	Natural Logarithm of HIRES_LENTIC_MEANSIZ
log_CONTACT	Natural Logarithm of CONTACT
log_STREAMS_KM_SQ_KM	Natural Logarithm of STREAMS_KM_SQ_KM
log_MAINSTEM_SINUOUSITY	Natural Logarithm of MAINSTEM_SINUOUSITY

2.5.4 Station Skew Map

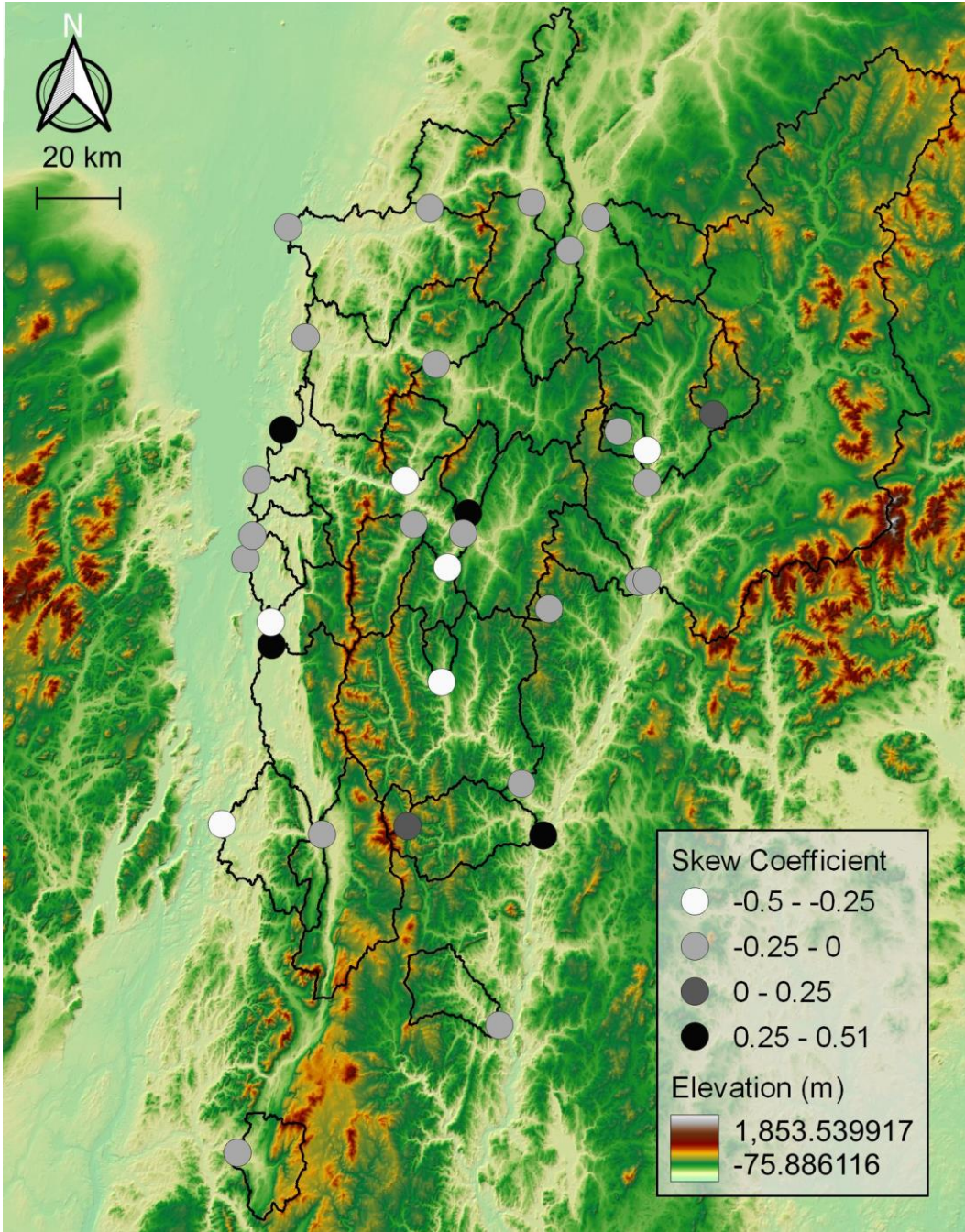


Figure 2-10 Estimated skew coefficient, K , of the flow frequency distribution at each gage analyzed.

2.5.5 CUAHSI Hydroshare Link

Many supplementary gage by gage figures are accessible on CUAHSI Hydroshare with the following URL,

<http://www.hydroshare.org/resource/24a49e928ada4a09b8eb5e1e984a1af8>

Chapter 3 | Concluding Remarks

The authors of the seminal textbook on FFA summarize the task of FFA as follows, “The practical issue is how to select a reasonable and simple distribution to describe the phenomenon of interest, to estimate that distribution’s parameters, and thus to obtain risk estimates of satisfactory accuracy for the problem at hand.”(Stedinger & Foufoula-Georgiou, 1993). That was the goal of this project, and I can only hope the preceding pages logged the process in as straightforward language. In reality, the process was much more meandering. The journey from first year graduate student to Master of Science involves a pay-as-you-go approach to learning with hours spent exploring the backwaters of scientific literature or deeply plunging into the mathematics of a method. At times when I questioned the scientific merit of developing a new statistical method. Did it enhance our understanding of the world, or was it too much of what Langbein (1958) called “tabulation, rearrangement, and fitting” without interpretation?

I’ve come to understand that characterizations of flow regime such as the one we developed here are what many hydrologists believe will be instrumental in advancing our science (Hrachowitz et al., 2013; McDonnell et al., 2007; Sivapalan, 2009). Further, I have hope that the method here described may be used to enable a richer coexistence of rivers and society, enabling a deeper understanding of river character and associated processes. The realization of such a project would have been in no way possible without the “course corrections” provided by my advisors, and to them I am deeply grateful.

We have succeeded in developing, applying, and interpreting the Duration-Over-Threshold model, an extension to the Peaks-Over-Threshold modeling approach that

relates the duration spent over a flowrate threshold to a recurrence interval. The problems that this model address span hydrologic subdisciplines from geomorphology to ecology and engineering, and it fills a niche that no other statistical FFA methods currently fill.

The Duration-Over-Threshold model is inspired by the model of Feng et al. (2017), but includes several notable changes. By using the partial duration series instead of the annual maxima, our model was able to properly model the frequency of frequent floods that drive many geomorphic and ecohydrological processes. The Duration-Over-Threshold model used discharge instead of stage records, allowing for regionalization of the model parameters and comparison of flow regime parameters across gauges. Our model was fit on higher-fidelity 15-minute data, which allowed for a more accurate characterization of flow regime, especially in smaller, flashier basins. We used a power law relationship between threshold flow rate and mean event duration, which was shown to be a better predictor than an exponential decay relationship at 31 of 33 USGS river gages within the state of Vermont. Tractable equations, open-source code, and documentation for the Duration-Over-Threshold model will make it more easily adopted by river practitioners.

For 26 gages, we developed regional regression equations to link model parameters to catchment- and reach-scale attributes. The regression equations enable model application in ungauged locations. A preliminary analysis of functional traits provided by the model found that flood duration tends to increase with drainage area but decreases in high-gradient streams and basins with low permeability soils.

Several model improvements could be pursued in the future. Seasonal analyses should be completed to separate out spring thaw dynamics, which are overwhelming the duration dynamics at low threshold flowrates (and such seasonal analyses have been enabled by the switch to POT frequency). The coefficient estimation within the regional regression analysis could be switched from OLS to GLS if a suitable covariance matrix is identified. Higher fidelity datasets on soils and land-cover could be used to improve regression performance and aid in duration process inference. Finally, a larger sample size (both in number of gages and length of record) could enable more accurate regionalization of the frequency skew coefficient.

Future efforts to extend the Duration-Over-Threshold model could involve deriving design flood hydrographs from the duration estimates. The data and parameters could easily be modified to model power-over-threshold or volume-over-threshold for geomorphic and detention structure modeling, respectively. If the threshold is set at some critical threshold for bed mobilization, toe scour, or bank erosion, and a damage function is constructed based on event duration, the frequency distribution may be used to estimate reach susceptibility to erosion. Stage-Duration relationships could be used for fluvial landform delineation or ecological gradient mapping. Lastly, comparative hydrology, functional trait, and machine-learning workflows may be used to link model parameters A and B (and other derived traits) to both causal and effective processes, revealing reproducible patterns in watershed function and deepening our understanding of watershed systems.

Comprehensive Bibliography

- Acosta, C. A., & Perry, S. A. (2001). Impact of hydropattern disturbance on crayfish population dynamics in the seasonal wetlands of Everglades National Park, USA. *Aquatic Conservation: Marine and Freshwater Ecosystems*, 11(1), 45-57. <https://doi.org/10.1002/aqc.426>
- Amini, S., Bidaki, R. Z., Mirabbasi, R., & Shafaei, M. (2022). Multivariate analysis of flood characteristics in Armand Watershed, Iran using vine copulas. *Arabian Journal of Geosciences*, 16(1), 11. <https://doi.org/10.1007/s12517-022-11102-5>
- Arias, M. E., Cochrane, T. A., Piman, T., Kumm, M., Caruso, B. S., & Killeen, T. J. (2012). Quantifying changes in flooding and habitats in the Tonle Sap Lake (Cambodia) caused by water infrastructure development and climate change in the Mekong Basin. *J Environ Manage*, 112, 53-66. <https://doi.org/10.1016/j.jenvman.2012.07.003>
- Armstrong, W. H., Collins, M. J., & Snyder, N. P. (2012). Increased Frequency of Low-Magnitude Floods in New England1 [<https://doi.org/10.1111/j.1752-1688.2011.00613.x>]. *JAWRA Journal of the American Water Resources Association*, 48(2), 306-320. <https://doi.org/https://doi.org/10.1111/j.1752-1688.2011.00613.x>
- Auble, G. T., Friedman, J. M., & Scott, M. L. (1994). Relating Riparian Vegetation to Present and Future Streamflows. *Ecological Applications*, 4(3), 544-554. <https://doi.org/10.2307/1941956>
- Bačová Mitková, V., & Halmová, D. (2014). Joint modeling of flood peak discharges, volume and duration: a case study of the Danube River in Bratislava. *Journal of Hydrology and Hydromechanics*, 62(3), 186-196. <https://doi.org/doi:10.2478/johh-2014-0026>
- Baker, G. L., & Gollub, J. P. (1996). *Chaotic Dynamics: An Introduction* (2 ed.). Cambridge University Press. <https://doi.org/DOI:10.1017/CBO9781139170864>
- Baustian, J. J., Piazza, B. P., & Bergan, J. F. (2019). Hydrologic connectivity and backswamp water quality during a flood in the Atchafalaya Basin, USA. *River Research and Applications*, 35(4), 430-435. <https://doi.org/10.1002/rra.3417>
- Bedinger, M. S. (1979). *Forest and flooding with special reference to the White River and Ouachita River basins, Arkansas* [Report](79-68). (Water-Resources Investigations Report, Issue. U. S. G. Survey. <http://pubs.er.usgs.gov/publication/wri7968>
- Benson, M. A. (1968). Uniform Flood-Frequency Estimating Methods for Federal Agencies. *Water Resources Research*, 4(5), 891-908. <https://doi.org/https://doi.org/10.1029/WR004i005p00891>
- Beven, K., & Wood, E. F. (1993). Flow Routing and the Hydrological Response of Channel Networks. In K. Beven & E. F. Wood (Eds.), *Channel Network Hydrology* (pp. 99-128).
- Chow, V. T., Maidment, D. R., & Mays, L. W. (1988). *Applied hydrology (chapter 5)*. McGraw-Hill New York.
- Coles, S. (2001). An Introduction to Statistical Modeling of Extreme Values. *Journal of the American Statistical Association*, 97, 1204 - 1204.
- Correia, F. N. (1987, 1987//). Multivariate Partial Duration Series in Flood Risk Analysis. Hydrologic Frequency Modeling, Dordrecht.

- Costa, J. E., & O'Connor, J. E. (1995). Geomorphically Effective Floods. In *Natural and Anthropogenic Influences in Fluvial Geomorphology* (pp. 45-56). <https://doi.org/https://doi.org/10.1029/GM089p0045>
- Cunderlik, J. M., & Ouarda, T. B. M. J. (2006). Regional flood-duration–frequency modeling in the changing environment. *Journal of Hydrology*, 318(1-4), 276-291. <https://doi.org/10.1016/j.jhydrol.2005.06.020>
- Dawdy, D. R., Griffis, V. W., & Gupta, V. K. (2012). Regional Flood-Frequency Analysis: How We Got Here and Where We Are Going. *Journal of Hydrologic Engineering*, 17(9), 953-959. [https://doi.org/10.1061/\(ASCE\)HE.1943-5584.0000584](https://doi.org/10.1061/(ASCE)HE.1943-5584.0000584)
- Devulapalli, R. S. (1995). *Flood volume-duration frequencies for ungaged rural catchments* (Publication Number 9534326) [Ph.D., Texas A&M University]. ProQuest Dissertations & Theses A&I. Ann Arbor. <https://login.ezproxy.uvm.edu/login?url=https://www.proquest.com/dissertations-theses/flood-volume-duration-frequencies-ungaged-rural/docview/304287531/se-2?accountid=14679>
- Diehl, R. M., Merritt, D. M., Wilcox, A. C., & Scott, M. L. (2017). Applying Functional Traits to Ecogeomorphic Processes in Riparian Ecosystems. *BioScience*, 67(8), 729-743. <https://doi.org/10.1093/biosci/bix080>
- Diehl, R. M., Wilcox, A. C., & Stella, J. C. (2020). Evaluation of the integrated riparian ecosystem response to future flow regimes on semiarid rivers in Colorado, USA. *J Environ Manage*, 271, 111037. <https://doi.org/10.1016/j.jenvman.2020.111037>
- Drobot, R., Draghia, A. F., Ciuiu, D., & Trandafir, R. (2021). Design floods considering the epistemic uncertainty. *Water*, 13(11), 1601.
- Duan, N. (1983). Smearing Estimate: A Nonparametric Retransformation Method. *Journal of the American Statistical Association*, 78(383), 605-610. <https://doi.org/10.2307/2288126>
- Dunne, T. (1978). Field Studies of Hillslope Flow Processes. *Hillslope Hydrol.*, 227.
- England Jr, J. F., Cohn, T. A., Faber, B. A., Stedinger, J. R., Thomas Jr, W. O., Veilleux, A. G., Kiang, J. E., & Mason, J. R. R. (2019). *Guidelines for determining flood flow frequency — Bulletin 17C* [Report](4-B5). (Techniques and Methods, Issue. U. S. G. Survey. <http://pubs.er.usgs.gov/publication/tm4B5>
- Falcone, J. A. (2011). *GAGES-II: Geospatial Attributes of Gages for Evaluating Streamflow* [Report]. U. S. G. Survey. <http://pubs.er.usgs.gov/publication/70046617>
- Favre, A.-C., El Adlouni, S., Perreault, L., Thiémondge, N., & Bobée, B. (2004). Multivariate hydrological frequency analysis using copulas [<https://doi.org/10.1029/2003WR002456>]. *Water Resources Research*, 40(1). <https://doi.org/https://doi.org/10.1029/2003WR002456>
- FEMA. (2006). *Hurricane Katrina in the Gulf Coast: Building Performance Observations, Recommendations, and Technical Guidance* (FEMA 549). https://www.preventionweb.net/files/1543_549cvrtoc1.pdf
- FEMA. (2019). *Guidance for Flood Risk Analysis and Mapping - General Hydrologic Considerations*. https://www.fema.gov/sites/default/files/2020-02/General_Hydrologic_Considerations_Guidance_Feb_2019.pdf
- Feng, Y., Brubaker, K. L., & McCuen, R. H. (2017). New View of Flood Frequency Incorporating Duration. *Journal of Hydrologic Engineering*, 22(11). [https://doi.org/10.1061/\(asce\)he.1943-5584.0001573](https://doi.org/10.1061/(asce)he.1943-5584.0001573)

- Ferreira, L. V., & Stohlgren, T. J. (1999). Effects of river level fluctuation on plant species richness, diversity, and distribution in a floodplain forest in Central Amazonia. *Oecologia*, 120(4), 582-587. <https://doi.org/10.1007/s004420050893>
- Frederick, R. H., Myers, V. A., & Auciello, E. P. (1977). Five- to 60-minute precipitation frequency for the eastern and central United States [Technical Memorandum]. <https://repository.library.noaa.gov/view/noaa/6435> (NOAA technical memorandum NWS HYDRO ; 35)
- Fuller, W. E. (1914). Flood Flows. *ASCE Trans*, 77, 567-617.
- Funk, J. L., Larson, J. E., Ames, G. M., Butterfield, B. J., Cavender-Bares, J., Firn, J., Laughlin, D. C., Sutton-Grier, A. E., Williams, L., & Wright, J. (2017). Revisiting the Holy Grail: using plant functional traits to understand ecological processes. *Biological Reviews*, 92(2), 1156-1173. <https://doi.org/https://doi.org/10.1111/brv.12275>
- Gaál, L., Szolgay, J., Kohnová, S., Parajka, J., Merz, R., Viglione, A., & Blöschl, G. (2012). Flood timescales: Understanding the interplay of climate and catchment processes through comparative hydrology. *Water Resources Research*, 48(4). <https://doi.org/https://doi.org/10.1029/2011WR011509>
- Ganguli, P., & Reddy, M. J. (2013). Probabilistic assessment of flood risks using trivariate copulas. *Theoretical and Applied Climatology*, 111(1), 341-360. <https://doi.org/10.1007/s00704-012-0664-4>
- Genest, C., & Favre, A.-C. (2007). Everything You Always Wanted to Know about Copula Modeling but Were Afraid to Ask. *Journal of Hydrologic Engineering*, 12(4), 347-368. [https://doi.org/10.1061/\(ASCE\)1084-0699\(2007\)12:4\(347\)](https://doi.org/10.1061/(ASCE)1084-0699(2007)12:4(347))
- Gervasi, A. A., Pasternack, G. B., & East, A. E. (2021). Flooding duration and volume more important than peak discharge in explaining 18 years of gravel–cobble river change [<https://doi.org/10.1002/esp.5230>]. *Earth Surface Processes and Landforms*, 46(15), 3194-3212. <https://doi.org/https://doi.org/10.1002/esp.5230>
- Goswami, M. (2022). Generating design flood hydrographs by parameterizing the characteristic flood hydrograph at a site using only flow data. *Hydrological Sciences Journal*, 67(16), 2505-2523. <https://doi.org/10.1080/02626667.2020.1843656>
- Hazen, A. (1930). *Flood Flows: A Study of Frequencies and Magnitudes*. J. Wiley & Sons, Incorporated. <https://books.google.com/books?id=Sn1EAAAAMAAJ>
- Hirsch, R. M., Helsel, D. R., Cohn, T. A., & Gilroy, E. J. (1993). Statistical Analysis of Hydrological Data. *Handbook of Hydrology*, 17.
- Hirschboeck, K. K., Ely, L. L., & Maddox, R. A. (2000). Hydroclimatology of Meteorologic Floods. In E. E. Wohl (Ed.), *Inland Flood Hazards: Human, Riparian, and Aquatic Communities* (pp. 39-72). Cambridge University Press. <https://doi.org/DOI:10.1017/CBO9780511529412.003>
- Hrachowitz, M., Savenije, H. H. G., Blöschl, G., McDonnell, J. J., Sivapalan, M., Pomeroy, J. W., Arheimer, B., Blume, T., Clark, M. P., Ehret, U., Fenicia, F., Freer, J. E., Gelfan, A., Gupta, H. V., Hughes, D. A., Hut, R. W., Montanari, A., Pande, S., Tetzlaff, D., . . . Cudennec, C. (2013). A decade of Predictions in Ungauged Basins (PUB)—a review. *Hydrological Sciences Journal*, 58(6), 1198-1255. <https://doi.org/10.1080/02626667.2013.803183>
- Hupp, C. R., & Osterkamp, W. R. (1985). Bottomland Vegetation Distribution along Passage Creek, Virginia, in Relation to Fluvial Landforms. *Ecology*, 66(3), 670-681. <https://doi.org/10.2307/1940528>

- Interagency Advisory Committee on Water Data. (1982). *Guidelines for Determining Flood Flow Frequency*.
- Javelle, P., Ouarda, T. B. M. J., & Bobée, B. (2003). Spring flood analysis using the flood-duration-frequency approach: application to the provinces of Quebec and Ontario, Canada. *Hydrological Processes*, 17(18), 3717-3736. <https://doi.org/10.1002/hyp.1349>
- Junk, W., Bayley, P., & Sparks, R. (1989). The Flood Pulse Concept in River-Floodplain Systems. In D. Dodge (Ed.), *Proceedings of the international large river symposium* (Vol. 106). Canadian Department of Fisheries and Oceans <https://publications.gc.ca/site/eng/9.816457/publication.html>
- Karim, F., Hasan, M., & Marvanek, S. (2017). Evaluating Annual Maximum and Partial Duration Series for Estimating Frequency of Small Magnitude Floods. *Water*, 9(7). <https://doi.org/10.3390/w9070481>
- Kennedy, J. R., Paretto, N. V., & Veilleux, A. G. (2015). *Methods for estimating magnitude and frequency of 1-, 3-, 7-, 15-, and 30-day flood-duration flows in Arizona* (2014-5109). (Scientific Investigations Report, Issue. U. S. G. Survey. <http://pubs.er.usgs.gov/publication/sir20145109>
- Kidson, R., & Richards, K. (2005). Flood Frequency Analysis: Assumptions and Alternatives. *Progress in Physical Geography - PROG PHYS GEOG*, 29, 392-410. <https://doi.org/10.1191/0309133305pp454ra>
- Lamontagne, J. R., Stedinger, J. R., Berenbrock, C., Veilleux, A. G., Ferris, J. C., & Knifong, D. L. (2012). *Development of regional skews for selected flood durations for the Central Valley Region, California, based on data through water year 2008* (2012-5130). (Scientific Investigations Report, Issue.
- Lang, M., Ouarda, T. B. M. J., & Bobée, B. (1999). Towards operational guidelines for over-threshold modeling. *Journal of Hydrology*, 225(3), 103-117. [https://doi.org/https://doi.org/10.1016/S0022-1694\(99\)00167-5](https://doi.org/https://doi.org/10.1016/S0022-1694(99)00167-5)
- Langbein, W. B. (1958). Divining Rods Versus Hydrologic Data and Research. *Journal of the Hydraulics Division*, 84(5), 1-6. <https://doi.org/10.1061/JYCEAJ.0000218>
- Leenman, A. S., Slater, L. J., Dadson, S. J., Wortmann, M., & Boothroyd, R. (2023). Quantifying the Geomorphic Effect of Floods Using Satellite Observations of River Mobility. *Geophysical Research Letters*, 50(16), e2023GL103875. <https://doi.org/https://doi.org/10.1029/2023GL103875>
- Lekach, J., & Enzel, Y. (2021). Flood-duration-integrated stream power and frequency magnitude of >50-year-long sediment discharge out of a hyperarid watershed. *Earth Surface Processes and Landforms*, 46(7), 1348-1362. <https://doi.org/10.1002/esp.5104>
- Magilligan, F. J., Buraas, E. M., & Renshaw, C. E. (2015). The efficacy of stream power and flow duration on geomorphic responses to catastrophic flooding. *Geomorphology*, 228, 175-188. <https://doi.org/10.1016/j.geomorph.2014.08.016>
- McDonnell, J. J., Sivapalan, M., Vaché, K., Dunn, S., Grant, G., Haggerty, R., Hinz, C., Hooper, R., Kirchner, J., Roderick, M. L., Selker, J., & Weiler, M. (2007). Moving beyond heterogeneity and process complexity: A new vision for watershed hydrology. *Water Resources Research*, 43(7). <https://doi.org/10.1029/2006wr005467>
- Merz, B., Kreibich, H., & Lall, U. (2013). Multi-variate flood damage assessment: a tree-based data-mining approach. *Nat. Hazards Earth Syst. Sci.*, 13(1), 53-64. <https://doi.org/10.5194/nhess-13-53-2013>

- Newcomer Johnson, T., Kaushal, S., Mayer, P., Smith, R., & Svirich, G. (2016). Nutrient Retention in Restored Streams and Rivers: A Global Review and Synthesis. *Water*, 8(4). <https://doi.org/10.3390/w8040116>
- Olson, S. A. (2002). *Flow-frequency characteristics of Vermont streams* (2002-4238). (Water-Resources Investigations Report, Issue. <http://pubs.er.usgs.gov/publication/wri024238>
- Olson, S. A. (2014). *Estimation of Flood Discharges at Selected Annual Exceedance Probabilities for Unregulated, Rural Streams in Vermont* (U.S. Geological Survey Scientific Investigations Report, Issue. <https://pubs.er.usgs.gov/publication/sir20145078>
- Ottino, J. M. (2003). Complex systems. *AIChE Journal*, 49(2), 292-299. <https://doi.org/https://doi.org/10.1002/aic.690490202>
- Pan, X., Rahman, A., Haddad, K., & Ouarda, T. B. M. J. (2022). Peaks-over-threshold model in flood frequency analysis: a scoping review. *Stochastic Environmental Research and Risk Assessment*. <https://doi.org/10.1007/s00477-022-02174-6>
- Pfurtscheller, C., & Schwarze, R. (2008). *Estimating the costs of emergency services during flood events* 4th International Symposium on Flood Defence, Toronto, ON.
- Razmkhah, H., Fararouie, A., & Ravari, A. R. (2022). Multivariate Flood Frequency Analysis Using Bivariate Copula Functions. *Water Resources Management*, 36(2), 729-743. <https://doi.org/10.1007/s11269-021-03055-3>
- Scott, D. T., Gomez-Velez, J. D., Jones, C. N., & Harvey, J. W. (2019). Floodplain inundation spectrum across the United States. *Nature Communications*, 10(1), 5194. <https://doi.org/10.1038/s41467-019-13184-4>
- Sherwood, J. M. (1994). *Estimation of peak-frequency relations, flood hydrographs, and volume-duration-frequency relations of ungaged small urban streams in Ohio* (2432). (Water Supply Paper, Issue. G. P. O. U.S. & I. S. For sale by the U.S. Geological Survey. <http://pubs.er.usgs.gov/publication/wsp2432>
- Sivapalan, M. (2003). Process complexity at hillslope scale, process simplicity at the watershed scale: is there a connection? *Hydrological Processes*, 17(5), 1037-1041. <https://doi.org/https://doi.org/10.1002/hyp.5109>
- Sivapalan, M. (2009). The secret to 'doing better hydrological science': change the question! *Hydrological Processes*, 23(9), 1391-1396. <https://doi.org/https://doi.org/10.1002/hyp.7242>
- Sivapalan, M., Blöschl, G., Zhang, L., & Vertessy, R. (2003). Downward approach to hydrological prediction. *Hydrological Processes*, 17(11), 2101-2111. <https://doi.org/https://doi.org/10.1002/hyp.1425>
- Smith, J. A. (1993). Precipitation. In D. R. Maidment (Ed.), *Handbook of Hydrology*. McGraw-Hill Education. https://books.google.com/books?id=4_9OAAAAMAAJ
- Soetanto, R., & Proverbs, D. G. (2004). Impact of flood characteristics on damage caused to UK domestic properties: the perceptions of building surveyors. *Structural Survey*, 22(2), 95-104. <https://doi.org/10.1108/02630800410538622>
- Sraj, M., Bezak, N., & Brilly, M. (2015). Bivariate flood frequency analysis using the copula function: a case study of the Litija station on the Sava River [<https://doi.org/10.1002/hyp.10145>]. *Hydrological Processes*, 29(2), 225-238. <https://doi.org/https://doi.org/10.1002/hyp.10145>
- Staff, S. S. (2023). *Soil Survey Geographic (SSURGO) Database* United States Department of Agriculture.

- Stedinger, J., & Foufoula-Georgiou, E. (1993). Frequency Analysis of Extreme Events. *Handbook of Hydrology*, 18.
- Survey, U. S. G. (2018). *USGS 1 arc-second n45w073 1 x 1 degree*. <https://www.usgs.gov/the-national-map-data-delivery>
- Survey, U. S. G. (2020). *USGS National Hydrography Dataset Plus High Resolution (NHDPlus HR) for 4-digit Hydrologic Unit - 0430*. <https://www.usgs.gov/national-hydrography/access-national-hydrography-products>
- Tasker, G. D., & Stedinger, J. R. (1989). An operational GLS model for hydrologic regression. *Journal of Hydrology*, 111(1-4), 361-375. <http://pubs.er.usgs.gov/publication/70015186>
- Thieken, A. H., Müller, M., Kreibich, H., & Merz, B. (2005). Flood damage and influencing factors: New insights from the August 2002 flood in Germany [<https://doi.org/10.1029/2005WR004177>]. *Water Resources Research*, 41(12). <https://doi.org/https://doi.org/10.1029/2005WR004177>
- Tosunoglu, F., Gürbüz, F., & İspirli, M. N. (2020). Multivariate modeling of flood characteristics using Vine copulas. *Environmental Earth Sciences*, 79(19), 459. <https://doi.org/10.1007/s12665-020-09199-6>
- USACE. (2022). *HEC-SSP*. In US Army Corps of Engineers. <https://www.hec.usace.army.mil/software/hec-ssp/>
- USEPA. (2008). *Methods for Evaluating Wetland Condition: Wetland Hydrology*. EPA-822-R-08-024.
- VTDEC. (2018). *State of Vermont Water Quality Integrated Assessment Report*. <https://dec.vermont.gov/content/2018-305b-water-quality-assessment-report>
- Ward, A., & Moran, M. (2016). A Novel Approach for Estimating the Recurrence Intervals of Channel-Forming Discharges. *Water*, 8(7). <https://doi.org/10.3390/w8070269>
- Wolman, M. G., & Miller, J. P. (1960). Magnitude and Frequency of Forces in Geomorphic Processes. *The Journal of Geology*, 68(1), 54-74. <https://doi.org/10.1086/626637>
- Yue, S., Ouarda, T. B. M. J., & Bobée, B. (2001). A review of bivariate gamma distributions for hydrological application. *Journal of Hydrology*, 246(1), 1-18. [https://doi.org/https://doi.org/10.1016/S0022-1694\(01\)00374-2](https://doi.org/https://doi.org/10.1016/S0022-1694(01)00374-2)